The University of Sydney

School of Civil Engineering
Sydney NSW 2006
AUSTRALIA

http://www.civil.usyd.edu.au/

Centre for Advanced Structural Engineering

Experimental Investigation of High Strength Cold-Formed C-Section in Combined Bending and Shear

Research Report No R894

Cao Hung Pham BE MConstMgt MEngSc
Gregory J Hancock BSc BE PhD DEng

April 2009

The University of Sydney

School of Civil Engineering
Centre for Advanced Structural Engineering
http://www.civil.usyd.edu.au/

Experimental Investigation of High Strength Cold-Formed C-Section in Combined Bending and Shear

Research Report No R894

Cao Hung Pham, BE, MConstMgt, MEngSc
Gregory J Hancock, BSc, BE, PhD, DEng
April 2009

Abstract:

In roof systems, high strength steel profiled sheeting fastened to high strength steel cold-formed purlins of lipped C or Z-section are commonly used throughout the world. The design of such systems is performed according to the provions of the limit states Australia/New Zealand Standard AS/NZS 4600:2005 (Standards Australia 2006) in Australia and the North American Specification (NAS) for the Design of Cold-Formed Steel Structural Members (AISI 2007) in the USA. In both Standards, which include the newly developed Direct Strength Method of design (DSM), the method presented [Chapter 7 of AS/NZS 4600:2005, Appendix 1 of (AISI 2007)] is limited to pure compression and pure bending. The situations of pure shear and combined bending and shear as occurs in a continuous purlin system are not considered.

In order to extend the DSM to purlin systems, three different test series on high strength cold-formed C-section purlins have been performed at the University of Sydney. The test series include predominantly shear, combined bending and shear and bending only test series. Two different section depths and three different thicknesses of lipped channel section were tested in this study. Further, tests with and without torsion/distortion restraint straps screwed on the top flanges adjacent to the loading points were also considered. This report summarizes the test results and formulae developed from the Effective Width Method (EWM) and Direct Strength Method of Design (DSM). Proposals for design are included in this report. Comparisons with AS 4100:1998 (Standards Australia 1998) are also included to take account of tension field action.

Keywords: Cold-formed; High strength steel; Direct strength method; Effective width method; Combined Bending and Shear; Shear Test; Tension Field Action.

Copyright Notice

School of Civil Engineering, Research Report R894

Experimental Investigation of High Strength Cold-Formed C-Section in Combined Bending and Shear

© 2009 Cao Hung Pham & Gregory J. Hancock
Email: C.Pham@usyd.edu.au
        hancock@eng.usyd.edu.au

ISSN 1833-2781

Published by:
School of Civil Engineering
The University of Sydney
Sydney NSW 2006
AUSTRALIA

April 2009

This report and other Research Reports published by the School of Civil Engineering are available on the Internet:

http://www.civil.usyd.edu.au

TABLE OF CONTENTS

LIST OF FIGURES

1 INTRODUCTION

High strength cold-formed steel sections are commonly used in a wide range of applications which include lipped C and Z-purlin sections in roof systems. Sections are normally made from high strength steel up to 550 MPa yield stress. With the resulting reduction of thicknesses of high strength steel, the failure modes of such sections are mainly due to instabilities such as local, distortional and flexural-torsional buckling modes or the interaction between them. In the cases of axial force and bending, the actions causing buckling such as flexural, flexural-torsional, distortional or local buckling, are well understood. However, for shear, the traditional approach has been to investigate shear plate buckling in the web alone and to ignore the behaviour of the whole section including the flanges. There does not appear to be any consistent theoretical or experimental investigation of the full section buckling of thin-walled sections under shear. Recently, Pham and Hancock (2009a) provided solutions to the shear buckling of complete channel sections loaded in pure shear parallel with the web by using a spline finite strip analysis (Lau and Hancock, 1986). For combined bending and shear, an extension to the DSM has been studied by Pham and Hancock (2009b). Eight different test series on purlin sheeting systems with single, double, and triple spans and both uplift and downwards load cases as well as screw and concealed-fastened sheeting were performed at the University of Sydney over a 10-year period. These test data were used to compare between the DSM and the EWM and to propose an extension to the DSM. Two approaches have been proposed and the calibration of the full set of vacuum rig test data was made to determine the limit states safety indices. The main purpose of this paper is to further refine the proposals based on tests which concentrated on shear, and combined bending and shear.

For cantilever beams and continuous beams, high bending and shear can act simultaneously at support points. The combination of shear stress and bending stress in a web produces a further reduction in the capacity of the web and the degree of the reduction depends upon whether the web is stiffened or not. In limit states design standards, the interaction is expressed in terms of bending moment and shear force so that the interaction formula for combined bending and shear of a section with an unstiffened web is given in Clause 3.3.5 of AS/NZS 4600 [Section C 3.3.2 of AISI (2007)] as:

$$\left(\frac{M^*}{M_s}\right)^2 + \left(\frac{V^*}{V_v}\right)^2 = 1 \qquad (1)$$

where M^* is bending action, M_s is the bending section capacity in pure bending, V^* is the shear action, and V_v is the shear capacity in pure shear. The interaction equation is shown in Fig. 1. This interaction is based upon an approximation to the theoretical interaction of local buckling resulting from shear and bending as derived by Timoshenko and Gere (1961).
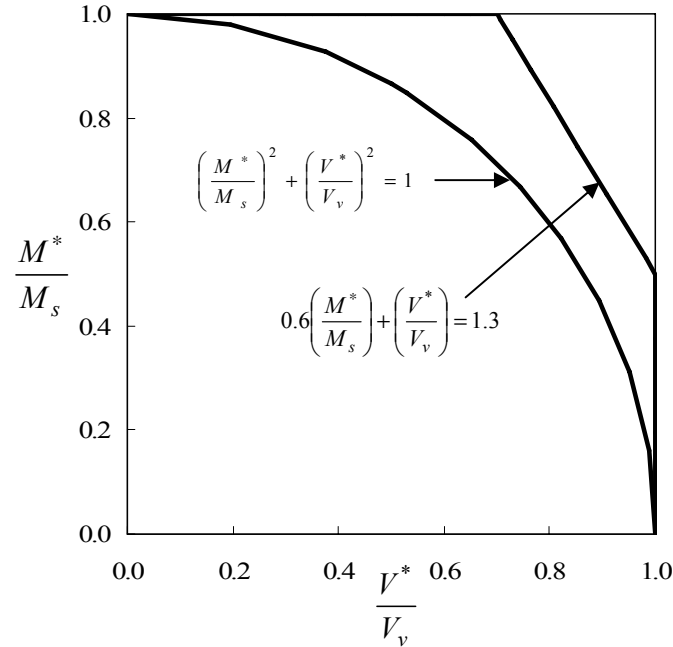
Figure 1. Interaction Relation for Bending and Shear

For a stiffened web, the interaction between shear and bending is not as severe, probably as a result of a greater postbuckling capacity in the combined bending and shear buckling mode. Eq. (1) was found to be conservative for beams with stiffened web due to the development of a diagonal tension field action. Based upon testing reported by LaBoube and Yu (1978), a linear relationship is given in Eq. (2) and also shown in Fig 1 with a larger permissible domain. The equation for combined bending and shear with stiffened webs is also given in Clause 3.3.5 of AS/NZS 4600 [Section C 3.3.2 of AISI (2007)] as:

$$0.6\left(\frac{M^*}{M_s}\right) + \frac{V^*}{V_v} = 1.3 \tag{2}$$

An experimental program was established at the University of Sydney to determine the ultimate strength of high strength cold-formed channel sections subjected to predominantly shear, combined bending and shear, and bending only. Two different depths and three different thicknesses were tested in the above series. The test results are plotted in this report as interaction diagrams where V_v and M_s are determined by different methods. For shear, V_v is based upon both Clause 3.3.4 of the Australian Cold-formed Steel Structures Standard AS/NZS 4600:2005 and Clause 5.11.5 of the Australian Steel Structures Standard AS 4100:1998 which includes tension field action. For bending, M_s is

computed by using either the EWM or DSM. This paper summarizes comparisons between the above approaches with test results. Recommendations for combined bending and shear in the DSM are included in the report.

2 EXPERIMENTAL INVESTIGATION

2.1 Test Series

The experimental program comprised a total of 60 tests which included three test series conducted in the J. W. Roderick Laboratory for Materials and Structures at the University of Sydney. All tests were performed in the 2000 kN capacity DARTEC testing machine, using a servo-controlled hydraulic ram. Two different commercially available lipped channel sections of 150 mm and 200 mm depths were chosen with three different thicknesses of 1.5 mm, 1.9 mm and 2.4 mm. The first series (*V*) is predominantly shear; and the second series (*MV*) is combined bending and shear. These series each consisted of twenty four tests and used the same test rig configuration. The third series is bending only (*M*) which used the common four point loading configuration. A total of twelve tests of this series were conducted. Although the tests described in LaBoube and Yu (1978) contained straps at the loading points as described later, tests both with and without straps are included in the test program described in this report.

2.1.1 Specimen Nomenclature and Dimensions

The test specimens were labeled in order to express the series, test number, channel section, depth and thickness. Typical test label "V1-C15015" is defined as follows:

- V indicates the predominantly shear test series. Alternatively, MV and M means the combined bending and shear series, and the bending only series respectively.
- "1" indicates the test number (alternatively "2", "3" and "w") where "w" expresses the test "without" straps adjacent to loading points or in the pure bending region.
- "C150" indicates a channel section (C-Section) with the web width of 150 mm (alternatively "C200").
- "15" is the thickness times 10 in mm (alternatively "19" and "24").

The average measured dimensions for the *V*, *MV* and *M* series are given in Tables 1(a), (b) and (c) respectively. In these tables, D is the overall depth, B is the average overall flange width, L is the overall lip depth and f_y is the average measured yield stress as described in Section 2.1.2. The Young's modulus of elasticity (E) was also calculated from stress-strain curves. The calculated mean value of the Young's modulus of elasticity is 206.9 GPa.

Test	Section	Thickness (mm)	D (mm)	B (mm)	L (mm)	f_y (MPa)
V1	C15015	1.5	153.39	64.78	15.68	541.13
V2	C15015	1.5	153.15	64.58	15.23	541.13
V3	C15015	1.5	153.37	64.38	14.19	541.13
Vw	C15015	1.5	153.22	64.64	15.48	541.13
V1	C15019	1.9	153.29	65.00	15.73	534.48
V2	C15019	1.9	153.41	64.60	15.58	534.48
V3	C15019	1.9	153.22	65.34	15.87	534.48
Vw	C15019	1.9	153.06	65.22	15.54	534.48
V1	C15024	2.4	153.40	62.96	17.68	485.29
V2	C15024	2.4	153.22	63.20	20.46	485.29
V3	C15024	2.4	153.49	62.67	19.55	485.29
Vw	C15024	2.4	153.06	63.04	17.52	485.29
V1	C20015	1.5	204.71	76.23	15.50	513.40
V2	C20015	1.5	204.55	76.72	15.65	513.40
V3	C20015	1.5	204.66	76.64	15.58	513.40
Vw	C20015	1.5	204.78	76.12	15.38	513.40
V1	C20019	1.9	202.22	78.16	16.90	510.48
V2	C20019	1.9	202.24	78.63	17.69	510.48
V3	C20019	1.9	201.93	78.70	17.63	510.48
Vw	C20019	1.9	201.96	78.14	16.88	510.48
V1	C20024	2.4	203.95	77.41	23.01	483.49
V2	C20024	2.4	203.35	77.73	22.15	483.49
V3	C20024	2.4	202.85	76.99	22.08	483.49

Internal Radius r = 5 mm

Table 1a. *V* Series Specimen Dimension and Properties

Test	Section	Thickness (mm)	D (mm)	B (mm)	L (mm)	f_y (MPa)
MV1	C15015	1.5	153.25	64.27	15.95	541.13
MV2	C15015	1.5	153.44	64.64	15.95	541.13
MV3	C15015	1.5	153.24	64.87	15.95	541.13
MVw	C15015	1.5	153.38	64.38	15.92	541.13
MV1	C15019	1.9	153.66	65.63	16.41	534.48
MV2	C15019	1.9	153.38	65.82	16.46	534.48
MV3	C15019	1.9	153.10	65.75	16.07	534.48
MVw	C15019	1.9	153.54	65.82	16.28	534.48
MV1	C15024	2.4	152.93	62.76	17.50	485.29
MV2	C15024	2.4	152.90	62.74	17.35	485.29
MV3	C15024	2.4	152.75	62.88	19.55	485.29
MVw	C15024	2.4	152.98	62.58	17.62	485.29
MV1	C20015	1.5	204.06	76.75	16.41	513.40
MV2	C20015	1.5	204.25	76.52	16.10	513.40
MV3	C20015	1.5	203.59	77.04	16.19	513.40
MVw	C20015	1.5	203.96	76.92	16.38	513.40
MV1	C20019	1.9	202.45	78.66	17.67	510.48
MV2	C20019	1.9	202.32	78.73	17.57	510.48
MV3	C20019	1.9	202.53	78.32	17.34	510.48
MVw	C20019	1.9	202.42	78.48	17.46	510.48
MV1	C20024	2.4	203.46	75.04	19.28	483.49
MV2	C20024	2.4	203.39	75.48	20.73	483.49
MV3	C20024	2.4	203.24	75.47	20.65	483.49
MVw	C20024	2.4	203.78	75.02	19.04	483.49

Internal Radius r = 5 mm

Table 1b. *MV* Series Specimen Dimension and Properties

Test	Section	Thickness (mm)	D (mm)	B (mm)	L (mm)	f_y (MPa)
M1	C15015	1.5	153.46	64.53	15.02	541.13
Mw	C15015	1.5	152.70	64.77	16.51	541.13
M1	C15019	1.9	153.54	65.01	16.27	534.48
Mw	C15019	1.9	153.38	64.47	16.00	534.48
M1	C15024	2.4	153.43	63.58	20.88	485.29
Mw	C15024	2.4	152.60	62.70	19.70	485.29
M1	C20015	1.5	203.74	75.88	16.16	513.40
Mw	C20015	1.5	203.70	76.08	16.42	513.40
M1	C20019	1.9	203.53	79.27	17.51	510.48
Mw	C20019	1.9	202.60	77.92	17.28	510.48
M1	C20024	2.4	202.30	77.58	21.26	483.49
Mw	C20024	2.4	203.35	76.61	20.88	483.49
Internal Radius r = 5 mm						

Table 1c. *M* Series Specimen Dimension and Properties

2.1.2 Specimen Nomenclature and Dimensions

Eighteen coupons were taken longitudinally from the centre of the web of each channel section member. The tensile coupon dimensions conformed to the Australian Standard AS 1391 (Standards Australia 1991) for the tensile testing of metals using 12.5 wide coupons with gauge length 50 mm.

The tests were performed using the 300 kN capacity Sintech/MTS 65/G testing machine operated in a displacement control mode. A constant displacement rate of 0.5 mm/min was maintained. The coupons were secured in a pair of vices and an extensometer was used to record the elongation. The extensometer has a range of 4.0 mm. Resetting the extensometer several times during test process allowed for the complete stress-strain curve to be determined. The yield stress f_y was obtained by using the 0.2 % nominal proof stress.

The coupons were identified by a label which indicates test specimen and coupon test number. For instance, "C15015-1" means the first coupon was cut longitudinally at the centre of the web of channel of a 150 mm depth and 1.5 mm thickness. Table 2 lists the details of every individual coupon test. The mean value for each purlin size and thickness is included in Table 2 and also in Tables 1a, 1b and 1c.

Specimen	b (mm)	A (mm²)	$f_{y0.2\%}$ (MPa)
C15015-1	12.33	18.50	540.58
C15015-2	12.45	18.68	536.46
C15015-3	12.34	18.51	546.36
		Mean	**541.13**
C15019-1	12.34	23.45	532.74
C15019-2	12.34	23.45	535.53
C15019-3	12.25	23.28	535.18
		Mean	**534.48**
C15024-1	12.36	29.66	491.99
C15024-2	12.34	29.62	478.73
C15024-3	12.36	29.66	485.14
		Mean	**485.29**
C20015-1	12.42	18.63	512.12
C20015-2	12.43	18.65	509.12
C20015-3	12.43	18.65	518.97
		Mean	**513.40**
C20019-1	12.42	23.60	506.84
C20019-2	12.40	23.56	513.61
C20019-3	12.40	23.56	510.99
		Mean	**510.48**
C20024-1	12.43	29.83	479.03
C20024-2	12.43	29.83	489.47
C20024-3	12.45	29.88	481.97
		Mean	**483.49**

Table 2. Coupon Test Results

2.2 Test Rig Design

2.2.1 *Test Set-Up 1* for Predominantly Shear *(V)* and Combined Bending and Shear Series *(MV)*

The basic design of the test rig was that developed by LaBoube and Yu (1978). A diagram of the test set-up is shown in Fig 2 for both the *V* and *MV* series. The only difference between the *V* and *MV* tests is the ratio of shear span to depth where the shear span is the distance between the lines of bolts at the loading and support points. With the *V* series, the ratio of span to depth is 1:1 whereas that of *MV* series is 2:1. The channel section members were tested in pairs with flanges facing inwards and with a gap between them to ensure inside assembly was possible. At the supports, the test two beam specimens were bolted through the webs by vertical rows of M12 high tensile bolts. These rows of bolts were connected to two channel sections 250x90x6CC with stiffeners. Steel plates of 20 mm thickness were used as load transfer plates which were also bolted through the flanges of the channel sections 250x90x6CC with stiffeners. These load bearing plates rested on the half rounds of the DARTEC supports to simulate a set of simple supports. At the loading point at mid-span, the DARTEC loading ram has a spherical head to ensure that the load is applied uniformly on the bearing plate, and moved at a constant stroke rate of 2 mm/min downwards during testing. The load was transferred to two channel sections 250x90x6CC with stiffeners which were connected to the test beam specimens by two vertical rows of M12 high tensile bolts. The distance between these two vertical rows of bolts is 50 mm. Further, the beam specimens were also connected by four 25x25x5EA equal angle steel straps on each top and

bottom flanges adjacent to the loading point and reactions. Self-tapping screws were used to attach these straps to the test specimens. The object of these straps was to prevent section distortion at the loading points.

The channel sections 250x90x6CC with stiffeners were introduced to prevent a bearing failure at the loading point and supports which could be caused by using conventional bearing plates. The complete fabrication details of the *V* and *MV* series are shown in Fig 2.
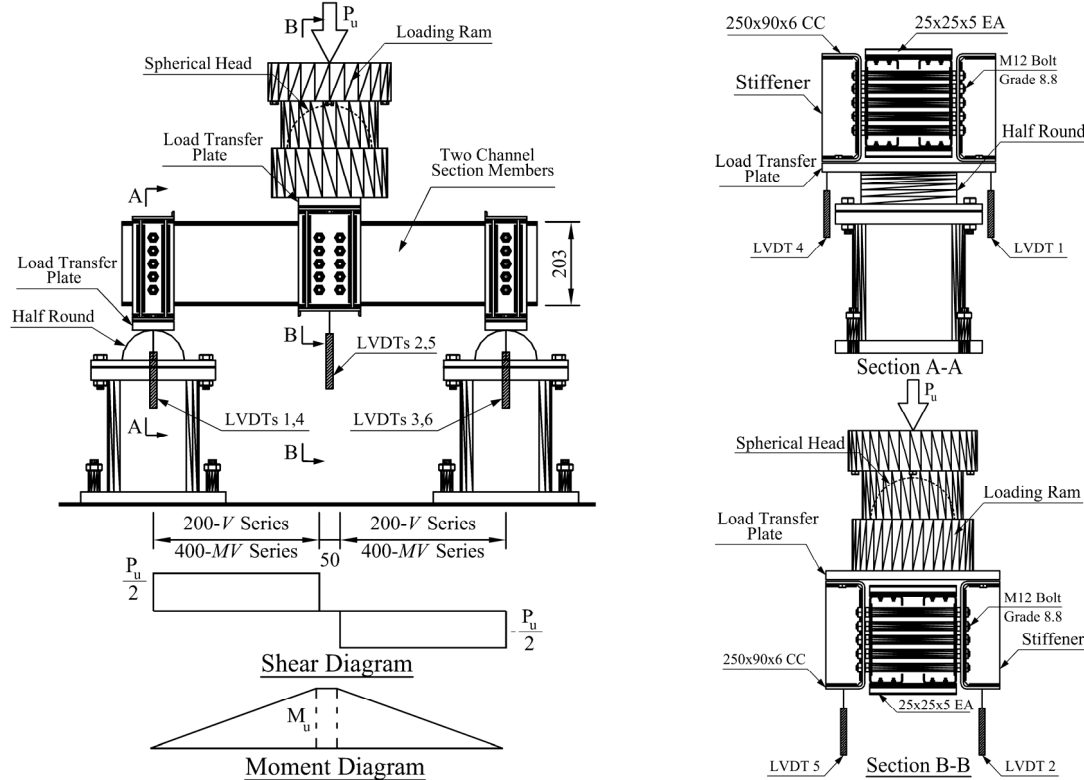
Figure 2. *V* and *MV* Test Series Configuration

2.2.2 *Test Set-Up 2* for Bending Only (M) Series

The detailed test configuration of bending only series is shown in Fig 3. The four point bending arrangement provided a central region of uniform bending moment and zero shear force. At the two supports, the rig assembly is exactly the same as that of the predominantly shear test set-up. The difference is at the loading points which have a similar configuration to the support points. The channel section members were loaded symmetrically at two points via a centrally loaded spreader I beam with stiffeners. The distance between the two half rounds bolted to the I beam at the loading points was 1000 mm. These two half rounds bore upon two 20 mm thick load transfer plates. The half round ensured that the applied loads were vertical. The distance between the support and the adjacent loading point was 800 mm.
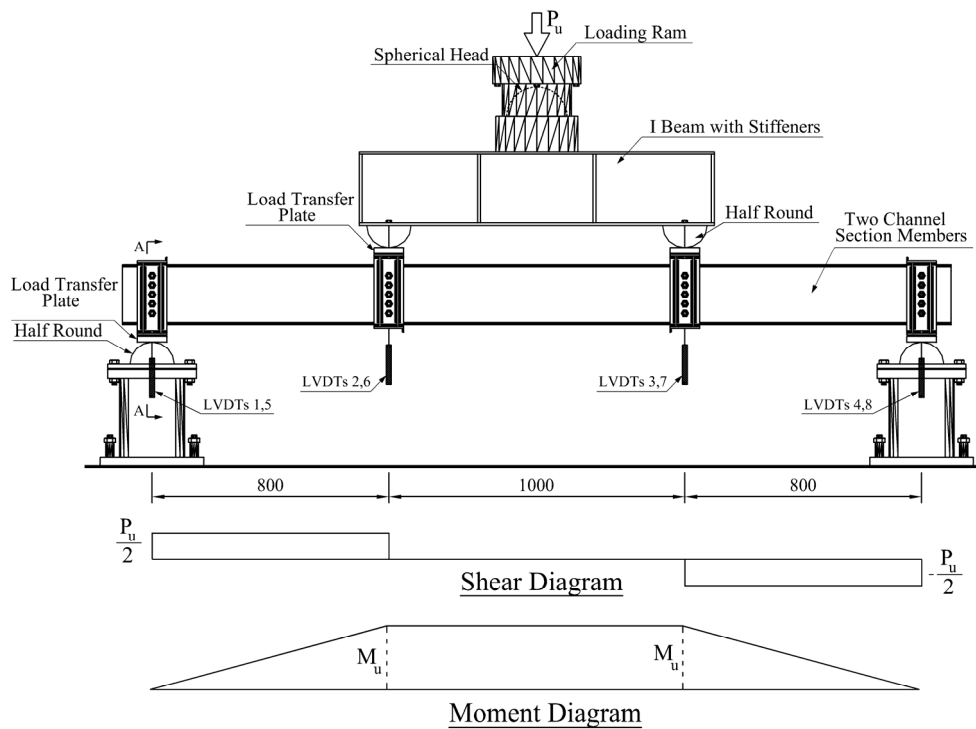
Figure 3. *M* Test Series Configuration

2.2.3 Tests With and Without Straps Configurations

For the predominantly shear *(V)* and the combined bending and shear *(MV)* test series, eighteen of the twenty four tests had four 25x25x5EA straps connected by self-tapping screws on each of the top and bottom flanges adjacent to the loading point and reactions as shown in Fig 4(a). Six remaining tests were tested without the two 25x25x5EA straps adjacent to the loading points on the top flange as shown in Fig 4(b). The purpose of these two straps is to prevent distortion of the top flanges under compression caused by bending moment. The distortion may be a consequence of unbalanced shear flow or distortional buckling.

(a) With Straps   (b) Without Straps
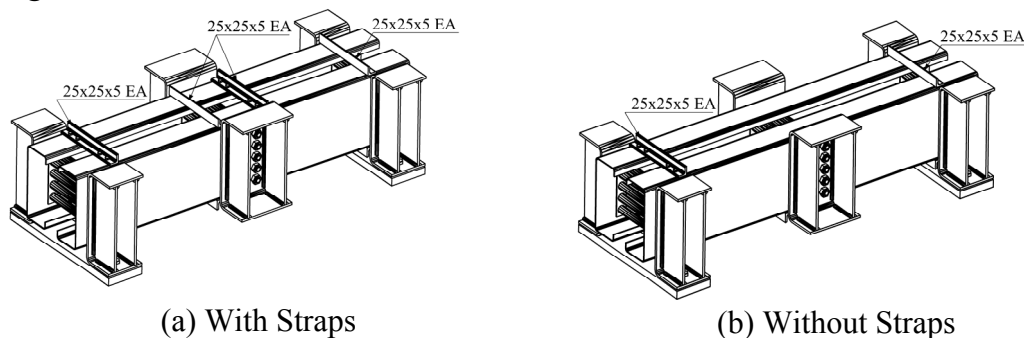
Figure 4. Combined Bending and Shear Test Series Configuration

For the bending only test series *(M)*, six of the twelve tests were tested with eight 25x25x5EA straps which were uniformly distributed in the pure bending moment region between the two loading points as shown in Fig 5(a). The

purpose of the straps is to force the channel members to buckle locally rather than by distortional buckling. The other six remaining tests in this series were tested without the six middle 25x25x5EA straps as shown in Fig 5(b). Only two straps adjacent to the loading points were attached to the channel members to prevent distortion at the loading points.

(a) With Straps   (b) Without Straps
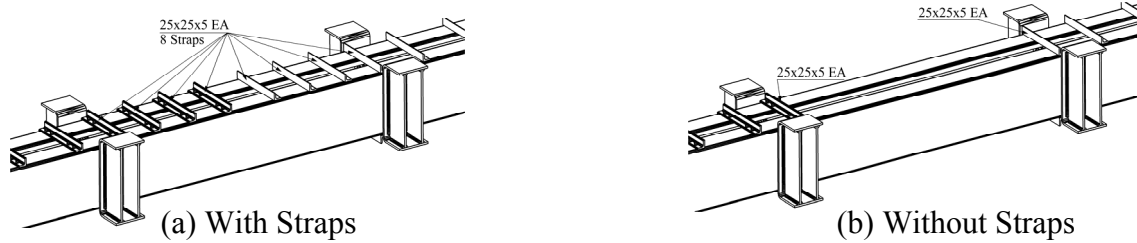
Figure 5. Bending only Test Series Configuration

3 EXPERIMENTAL RESULTS

The results of the tests for predominantly the shear *(V)*, the combined bending and shear *(MV)* and the bending only test series are shown in Tables 3a, 3b and 3c respectively. They include the full load (P_T) applied through the loading head on both purlins, and the shear span (s).The ratios *(M_T/M_M)* of bending moment to maximum bending moment for the 4 tests of a given size in all 3 test series and the ratios *(V_T/V_M)* of shear force to maximum shear force for the 4 tests of a given size in all 3 test series are also included in these tables.

Test	Section	s (mm)	P_T (kN)	$M_T = \dfrac{P_T * s}{4}$ (kNm)	$V_T = \dfrac{P_T}{4}$ (kN)	$\dfrac{M_T}{M_M}$	$\dfrac{V_T}{V_V}$
V1	C15015	150	221.71	8.31	55.43	0.797	0.988
V2	C15015	150	224.33	8.41	56.08	0.807	1.000
V3	C15015	150	217.86	8.17	54.47	0.784	0.971
Vw	C15015	150	205.10	7.69	51.28	0.738	0.914
V1	C15019	150	307.10	11.52	76.78	0.726	0.986
V2	C15019	150	302.59	11.35	75.65	0.715	0.972
V3	C15019	150	311.38	11.68	77.85	0.736	1.000
Vw	C15019	150	283.48	10.63	70.87	0.670	0.910
V1	C15024	150	376.94	14.14	94.24	0.713	0.981
V2	C15024	150	384.14	14.41	96.04	0.726	1.000
V3	C15024	150	382.23	14.33	95.56	0.723	0.995
Vw	C15024	150	373.52	14.01	93.38	0.706	0.972
V1	C20015	200	224.58	11.23	56.14	0.834	0.972
V2	C20015	200	215.54	10.78	53.89	0.800	0.933
V3	C20015	200	231.05	11.55	57.76	0.858	1.000
Vw	C20015	200	203.27	10.16	50.82	0.755	0.880
V1	C20019	200	346.05	17.30	86.51	0.795	1.000
V2	C20019	200	344.22	17.21	86.06	0.791	0.995
V3	C20019	200	333.54	16.68	83.38	0.767	0.964
Vw	C20019	200	303.26	15.16	75.82	0.697	0.876
V1	C20024	200	461.79	23.09	115.45	0.736	1.000
V2	C20024	200	454.40	22.72	113.60	0.724	0.984
V3	C20024	200	450.43	22.52	112.61	0.718	0.975
Vw	C20024	200	413.26	20.66	103.31	0.658	0.895

Table 3a. *V* Series Test Results

Test	Section	s (mm)	P_T (kN)	$M_T = \dfrac{P_T * s}{4}$ (kNm)	$V_T = \dfrac{P_T}{4}$ (kN)	$\dfrac{M_T}{M_M}$	$\dfrac{V_T}{V_V}$
MV1	C15015	300	142.96	10.72	35.74	1.028	0.637
MV2	C15015	300	134.11	10.06	33.53	0.965	0.598
MV3	C15015	300	141.80	10.64	35.45	1.020	0.632
MVw	C15015	300	107.19	8.04	26.80	0.771	0.478
MV1	C15019	300	197.35	14.80	49.34	0.933	0.634
MV2	C15019	300	187.89	14.09	46.97	0.889	0.603
MV3	C15019	300	195.22	14.64	48.80	0.923	0.627
MVw	C15019	300	153.64	11.52	38.41	0.727	0.493
MV1	C15024	300	253.82	19.04	63.45	0.960	0.661
MV2	C15024	300	263.03	19.73	65.76	0.994	0.685
MV3	C15024	300	251.07	18.83	62.77	0.949	0.654
MVw	C15024	300	216.70	16.25	54.18	0.819	0.564
MV1	C20015	400	139.66	13.97	34.92	1.037	0.604
MV2	C20015	400	128.68	12.87	32.17	0.956	0.557
MV3	C20015	400	142.23	14.22	35.56	1.056	0.616
MVw	C20015	400	97.00	9.70	24.25	0.720	0.420
MV1	C20019	400	222.81	22.28	55.70	1.024	0.644
MV2	C20019	400	218.47	21.85	54.62	1.004	0.631
MV3	C20019	400	212.80	21.28	53.20	0.978	0.615
MVw	C20019	400	159.20	15.92	39.80	0.732	0.460
MV1	C20024	400	294.04	29.40	73.51	0.937	0.637
MV2	C20024	400	289.04	28.90	72.26	0.921	0.626
MV3	C20024	400	286.54	28.65	71.63	0.913	0.620
MVw	C20024	400	221.22	22.12	55.30	0.705	0.479

Table 3b. *MV* Series Test Results

Test	Section	s (mm)	P_T (kN)	$M_T = \dfrac{P_T * s}{4}$ (kNm)	$V_T = \dfrac{P_T}{4}$ (kN)	$\dfrac{M_T}{M_M}$	$\dfrac{V_T}{V_V}$
M1	C15015	800	52.13	10.43	13.03	1.000	0.232
Mw	C15015	800	47.37	9.47	11.84	0.909	0.211
M1	C15019	800	79.30	15.86	19.82	1.000	0.255
Mw	C15019	800	64.71	12.94	16.18	0.816	0.208
M1	C15024	800	99.19	19.84	24.80	1.000	0.258
Mw	C15024	800	88.82	17.76	22.20	0.895	0.231
M1	C20015	800	67.33	13.47	16.83	1.000	0.291
Mw	C20015	800	60.98	12.20	15.25	0.906	0.264
M1	C20019	800	108.78	21.76	27.20	1.000	0.314
Mw	C20019	800	94.25	18.85	23.56	0.866	0.272
M1	C20024	800	156.94	31.39	39.24	1.000	0.340
Mw	C20024	800	139.42	27.88	34.86	0.888	0.302

Table 3c. *M* Series Test Results

4 DESIGN CRITERIA FOR PURLINS SYSTEMS

4.1 Nominal Shear Capacity based on AS/NZS 4600:2005

The nominal shear capacity (V_v) of a web is calculated from Section 3.3.4.1 of AS/NZS 4600:2005 in DSM format as follows:

$$\text{For } \lambda_v \leq 0.841: V_v = V_y \tag{3}$$

$$\text{For } 0.841 < \lambda_v \leq 1.191: V_v = 0.841\sqrt{V_{cr}V_y} \tag{4}$$

$$\text{For } \lambda_v > 1.191: V_v = V_{cr} \tag{5}$$

where $\lambda_v = \sqrt{V_y / V_{cr}}$

V_y = yield load of web = $0.64 A_w f_y$

V_{cr} = elastic shear buckling force of web = $\dfrac{k_v \pi^2 E A_w}{12\left(1 - v^2\right)\left(\dfrac{d_1}{t_w}\right)^2}$

d_1 = depth of the flat portion of the web measured along the plane of the web

t_w = thickness of web

A_w = area of web = $d_1 \times t_w$

k_v = shear buckling coefficient: $k_v = 5.34$ for unstiffened webs

4.2 Nominal Shear Capacity based on the Australian Steel Structures AS 4100:1998 with Tension Field

The nominal shear capacity (V_v) of a web where the shear stress distribution is approximately uniform is calculated from Section 5.11.2 of AS 4100-1998 as follows:

$$V_v = V_u \tag{6}$$

where V_u is the nominal shear capacity of the web with a uniform shear stress distribution given as follows:

(a) When the maximum web panel depth to thickness ratio d_1/t_w satisfies

$$\frac{d_1}{t_w} \leq \frac{82}{\sqrt{\left(\dfrac{f_y}{250}\right)}}$$

the nominal shear capacity of the web (V_u) is calculated as follows

$$V_u = V_w$$

where the nominal shear yield capacity of the web is $V_w = 0.6 f_y A_w$ specified in Section 5.11.4

(b) When the maximum web panel depth to thickness ratio d_1/t_w satisfies

$$\frac{d_1}{t_w} > \frac{82}{\sqrt{\left(\frac{f_y}{250}\right)}}$$

the nominal shear capacity of the web (V_u) is calculated as follows

$$V_u = V_b$$

where the nominal shear yield capacity of the web is (V_b) specified in Section 5.11.5

Unstiffened Web: The nominal shear buckling capacity (V_b) for an unstiffened web or a web considered to be unstiffened is calculated as follows:

$$V_b = \alpha_v V_w$$

where $\alpha_v = \left[\dfrac{82}{\left(\dfrac{d_1}{t_w}\right)\sqrt{\left(\dfrac{f_y}{250}\right)}}\right]$

Stiffened Web: The nominal shear buckling capacity (V_b) for a stiffened web with s/d_1 is calculated as follows:

$$V_b = \alpha_v \alpha_d V_w$$

where $\alpha_v = \left[\dfrac{82}{\left(\dfrac{d_1}{t_w}\right)\sqrt{\left(\dfrac{f_y}{250}\right)}}\right]^2 \left[\dfrac{0.75}{\left(\dfrac{s}{d_1}\right)}+1\right] \le 1.0$ when $1.0 \le s/d_1 \le 3$

$\alpha_v = \left[\dfrac{82}{\left(\dfrac{d_1}{t_w}\right)\sqrt{\left(\dfrac{f_y}{250}\right)}}\right]^2 \left[\dfrac{1}{\left(\dfrac{s}{d_1}\right)^2}+0.75\right] \le 1.0$ when $s/d_1 \le 1.0$

$\alpha_d = 1 + \dfrac{1-\alpha_v}{1.15\alpha_v\sqrt{\left[1+\left(\dfrac{s}{d_1}\right)^2\right]}}$

s = spacing of stiffeners

In the tests described in this paper, the stiffener spacing, s, is the same as the shear span distance between lines of vertical bolts which can be regarded as stiffened points.

4.3 Nominal Section Moment Capacity based on the EWM

The nominal section moment capacity *(M$_s$)* is determined as follows:

$$M_s = Z_e f_y \tag{7}$$

where Z_e = section modulus about a horizontal axis of the effective section.

4.4 Nominal Section Moment Capacity based on the DSM

4.4.1 Nominal Section Moment Capacity at Local Buckling *(M$_{sl}$)*

The nominal section moment capacity at local buckling *(M$_{sl}$)* is determined from Section 7.2.2.3 of AS/NZS 4600:2005 [Appendix 1, Section 1.2.2.2 of NAS (2005)] as follows:

$$\text{For } \lambda_l \leq 0.776: \ M_{sl} = M_y \tag{8}$$

$$\text{For } \lambda_l > 0.776: \ M_{sl} = \left[1 - 0.15\left(\frac{M_{ol}}{M_y}\right)^{0.4}\right]\left(\frac{M_{ol}}{M_y}\right)^{0.4} M_y \tag{9}$$

where λ_l = non-dimensional slenderness used to determine M_{sl}

$\quad = \sqrt{M_y / M_{ol}}$

$M_y = Z_f f_y$

M_{ol} = elastic local buckling moment of the section.

$\quad = Z_f f_{ol}$

Z_f = section modulus about a horizontal axis of the full section.

f_{ol} = elastic local buckling stress of the section in bending.

4.4.2 Nominal Section Moment Capacity at Distortional Buckling *(M$_{sd}$)*

The nominal section moment capacity at distortional buckling *(M$_{sd}$)* is determined from Section 7.2.2.4 of AS/NZS 4600:2005 [Appendix 1, Section 1.2.2.3 of NAS (2005)] as follows:

$$\text{For } \lambda_d \leq 0.673: \ M_{sd} = M_y \tag{10}$$

$$\text{For } \lambda_d > 0.673: \ M_{sd} = \left[1 - 0.22\left(\frac{M_{od}}{M_y}\right)^{0.5}\right]\left(\frac{M_{od}}{M_y}\right)^{0.5} M_y \tag{11}$$

where λ_d = non-dimensional slenderness used to determine M_{sd}

$$= \sqrt{M_y / M_{od}}$$

M_{od} = elastic distortional buckling moment of the section.

$$= Z_f f_{od}$$

$M_y = Z_f f_y$

Z_f = section modulus about a horizontal axis of the full section.

f_{od} = elastic distortional buckling stress of the section in bending.

5 COMPARISONS OF TEST RESULTS WITH EWM AND DSM DESIGN LOADS

The results of tests for the predominantly shear *(V)*, the combined bending and shear *(MV)* and the bending only *(M)* test series respectively are summarized in Tables 4a, 4b and 4c as are the test moments *(M_T)* non-dimensionalized with respect to the EWM capacities *(M_s)*. For the DSM, the nominal section moment capacities at local buckling *(M_{sl})* and at distortional buckling *(M_{sd})* are shown in Tables 5a, 5b and 5c as are the test moments non-dimensionalized with respect to these. The elastic local buckling stresses *(f_{ol})* and distortional buckling stresses *(f_{od})*, the elastic local buckling moment *(M_{ol})* and distortional buckling moment *(M_{od})* are given in Appendices 1-3.

For the nominal shear capacities, V_v, Section 3.3.4.1 of AS/NZS 4600:2005 for Australian Cold-Formed Steel Structures in DSM format [V_v (AS4600)] and Section 5.11.2 of AS 4100-1998 [V_v (AS4100)] with the tension field effect have been utilized. The test values, V_T, have been non-dimensionalized with respect to both these values. All the calculations have been based on the test values of yield stress *(f_y)* and the measured dimensions to provide a true measure of design model accuracy. The interactions between *(M_T/M_s)* and *(V_T/V_v)* with and without the straps based on either AS/NZS 4600:2005 or AS 4100-1998 are graphically reproduced in Figs. 7-8 for the EWM and in Figs 9-12 for the DSM.

Test	Section	M_T (kNm)	V_T (kN)	$M_s = Z_e f_y$ (kNm)	$\dfrac{M_T}{M_s}$	V_v (AS4600) (kN)	$\dfrac{V_T}{V_{v(AS4600)}}$	V_v (AS4100) (kN)	$\dfrac{V_T}{V_{v(AS4100)}}$
V1	C15015	8.31	55.43	9.09	0.915	40.59	1.366	56.93	0.974
V2	C15015	8.41	56.08	9.00	0.934	40.66	1.379	56.85	0.986
V3	C15015	8.17	54.47	8.86	0.922	40.59	1.342	56.92	0.957
Vw	C15015	7.69	51.28	9.05	0.850	40.64	1.262	56.88	0.902
V1	C15019	11.52	76.78	11.85	0.971	72.96	1.052	83.67	0.918
V2	C15019	11.35	75.65	11.82	0.960	72.96	1.037	83.71	0.904
V3	C15019	11.68	77.85	11.88	0.983	72.96	1.067	83.65	0.931
Vw	C15019	10.63	70.87	11.81	0.900	72.96	0.971	83.60	0.848
V1	C15024	14.14	94.24	14.92	0.947	103.31	0.912	96.86	0.973
V2	C15024	14.41	96.04	15.53	0.927	103.18	0.931	96.73	0.993
V3	C15024	14.33	95.56	15.34	0.934	103.38	0.924	96.92	0.986
Vw	C15024	14.01	93.38	14.85	0.944	103.06	0.906	96.62	0.966
V1	C20015	11.23	56.14	11.81	0.951	29.72	1.889	65.25	0.860
V2	C20015	10.78	53.89	11.83	0.911	29.75	1.811	65.19	0.827
V3	C20015	11.55	57.76	11.82	0.977	29.73	1.943	65.23	0.886
Vw	C20015	10.16	50.82	11.78	0.863	29.71	1.710	65.27	0.779
V1	C20019	17.30	86.51	17.60	0.983	61.46	1.408	90.07	0.960
V2	C20019	17.21	86.06	17.80	0.967	61.45	1.400	90.08	0.955
V3	C20019	16.68	83.38	17.75	0.939	61.55	1.355	89.96	0.927
Vw	C20019	15.16	75.82	17.57	0.863	61.54	1.232	89.97	0.843
V1	C20024	23.09	115.45	23.98	0.963	110.72	1.043	128.26	0.900
V2	C20024	22.72	113.60	23.71	0.958	110.72	1.026	128.03	0.887
V3	C20024	22.52	112.61	23.55	0.956	110.72	1.017	127.84	0.881
Vw	C20024	20.66	103.31	24.11	0.857	110.72	0.933	128.32	0.805

Table 4a. *V* Series Test Results with
M_s based on EWM, V_v based on AS4600 and AS4100

Test	Section	M_T (kNm)	V_T (kN)	$M_s = Z_e f_y$ (kNm)	$\dfrac{M_T}{M_s}$	V_v (AS4600) (kN)	$\dfrac{V_T}{V_{v(AS4600)}}$	V_v (AS4100) (kN)	$\dfrac{V_T}{V_{v(AS4100)}}$
MV1	C15015	10.72	35.74	9.11	1.177	27.58	1.296	43.00	0.831
MV2	C15015	10.06	33.53	9.13	1.102	27.54	1.217	43.03	0.779
MV3	C15015	10.64	35.45	9.12	1.166	27.58	1.285	43.00	0.824
MVw	C15015	8.04	26.80	9.12	0.882	27.55	0.973	43.02	0.623
MV1	C15019	14.80	49.34	12.02	1.231	56.20	0.878	67.70	0.729
MV2	C15019	14.09	46.97	12.01	1.173	56.32	0.834	67.67	0.694
MV3	C15019	14.64	48.80	11.92	1.228	56.43	0.865	67.65	0.721
MVw	C15019	11.52	38.41	12.00	0.960	56.25	0.683	67.69	0.567
MV1	C15024	19.04	63.45	14.82	1.285	91.39	0.694	96.53	0.657
MV2	C15024	19.73	65.76	14.78	1.335	91.39	0.720	96.51	0.681
MV3	C15024	18.83	62.77	15.25	1.235	91.39	0.687	96.40	0.651
MVw	C15024	16.25	54.18	14.85	1.095	91.39	0.593	96.56	0.561
MV1	C20015	13.97	34.92	11.98	1.166	20.24	1.725	46.13	0.757
MV2	C20015	12.87	32.17	11.92	1.079	20.22	1.591	46.18	0.697
MV3	C20015	14.22	35.56	11.91	1.195	20.29	1.752	46.02	0.773
MVw	C20015	9.70	24.25	11.97	0.811	20.25	1.197	46.11	0.526
MV1	C20019	22.28	55.70	17.81	1.251	41.67	1.337	67.64	0.824
MV2	C20019	21.85	54.62	17.77	1.229	41.70	1.310	67.61	0.808
MV3	C20019	21.28	53.20	17.73	1.200	41.65	1.277	67.66	0.786
MVw	C20019	15.92	39.80	17.75	0.897	41.67	0.955	67.63	0.588
MV1	C20024	29.40	73.51	22.93	1.283	83.98	0.875	102.97	0.714
MV2	C20024	28.90	72.26	23.27	1.242	84.01	0.860	102.96	0.702
MV3	C20024	28.65	71.63	23.23	1.234	84.07	0.852	102.94	0.696
MVw	C20024	22.12	55.30	22.92	0.965	83.83	0.660	103.01	0.537

Table 4b. *MV* Series Test Results with
M_s based on EWM, V_v based on AS4600 and AS4100

Test	Section	M_T (kNm)	V_T (kN)	$M_s = Z_e f_y$ (kNm)	$\dfrac{M_T}{M_s}$	V_v (AS4600) (kN)	$\dfrac{V_T}{V_{v(AS4600)}}$	V_v (AS4100) (kN)	$\dfrac{V_T}{V_{v(AS4100)}}$
M1	C15015	10.43	13.03	8.99	1.160	23.19	0.562	24.23	0.538
Mw	C15015	9.47	11.84	9.16	1.034	23.32	0.508	24.37	0.486
M1	C15019	15.86	19.82	11.96	1.326	47.38	0.418	49.51	0.400
Mw	C15019	12.94	16.18	11.88	1.090	47.43	0.341	49.56	0.326
M1	C15024	19.84	24.80	15.67	1.266	83.88	0.296	96.88	0.256
Mw	C15024	17.76	22.20	15.26	1.164	83.88	0.265	96.30	0.231
M1	C20015	13.47	16.83	11.90	1.132	17.08	0.986	17.85	0.943
Mw	C20015	12.20	15.25	11.95	1.020	17.08	0.892	17.85	0.854
M1	C20019	21.76	27.20	17.87	1.218	34.90	0.779	36.46	0.746
Mw	C20019	18.85	23.56	17.71	1.064	35.07	0.672	36.64	0.643
M1	C20024	31.39	39.24	23.32	1.346	71.17	0.551	74.36	0.528
Mw	C20024	27.88	34.86	23.35	1.194	70.77	0.493	73.95	0.471

Table 4c. *M* Series Test Results with
M_s based on EWM, V_v based on AS4600 and AS4100

Test	Section	M_T (kNm)	V_T (kN)	M_{sl} (kNm)	M_{sd} (kNm)	$\dfrac{M_T}{M_{sl}}$	$\dfrac{M_T}{M_{sd}}$	V_v (AS4600) (kN)	$\dfrac{V_T}{V_{v(AS4600)}}$	V_v (AS4100) (kN)	$\dfrac{V_T}{V_{v(AS4100)}}$
V1	C15015	8.31	55.43	9.61	7.81	0.865	1.064	40.59	1.366	56.93	0.974
V2	C15015	8.41	56.08	9.56	7.70	0.880	1.093	40.66	1.379	56.85	0.986
V3	C15015	8.17	54.47	9.49	7.47	0.861	1.094	40.59	1.342	56.92	0.957
Vw	C15015	7.69	51.28	9.59	7.76	0.802	0.992	40.64	1.262	56.88	0.902
V1	C15019	11.52	76.78	13.90	10.79	0.829	1.068	72.96	1.052	83.67	0.918
V2	C15019	11.35	75.65	13.86	10.74	0.819	1.056	72.96	1.037	83.71	0.904
V3	C15019	11.68	77.85	13.93	10.82	0.838	1.079	72.96	1.067	83.65	0.931
Vw	C15019	10.63	70.87	13.87	10.72	0.766	0.992	72.96	0.971	83.60	0.848
V1	C15024	14.14	94.24	16.40	14.46	0.862	0.978	103.31	0.912	96.86	0.973
V2	C15024	14.41	96.04	16.70	15.20	0.862	0.948	103.18	0.931	96.73	0.993
V3	C15024	14.33	95.56	16.56	14.96	0.866	0.958	103.38	0.924	96.92	0.986
Vw	C15024	14.01	93.38	16.35	14.38	0.857	0.974	103.06	0.906	96.62	0.966
V1	C20015	11.23	56.14	12.73	10.43	0.882	1.076	29.72	1.889	65.25	0.860
V2	C20015	10.78	53.89	12.77	10.47	0.844	1.029	29.75	1.811	65.19	0.827
V3	C20015	11.55	57.76	12.76	10.46	0.905	1.105	29.73	1.943	65.23	0.886
Vw	C20015	10.16	50.82	12.71	10.40	0.800	0.978	29.71	1.710	65.27	0.779
V1	C20019	17.30	86.51	18.84	14.97	0.918	1.156	61.46	1.408	90.07	0.960
V2	C20019	17.21	86.06	18.98	15.27	0.907	1.127	61.45	1.400	90.08	0.955
V3	C20019	16.68	83.38	18.96	15.23	0.880	1.095	61.55	1.355	89.96	0.927
Vw	C20019	15.16	75.82	18.81	14.94	0.806	1.015	61.54	1.232	89.97	0.843
V1	C20024	23.09	115.45	27.40	22.85	0.843	1.011	110.72	1.043	128.26	0.900
V2	C20024	22.72	113.60	27.26	22.47	0.834	1.011	110.72	1.026	128.03	0.887
V3	C20024	22.52	112.61	27.08	22.34	0.832	1.008	110.72	1.017	127.84	0.881
Vw	C20024	20.66	103.31	27.52	23.01	0.751	0.898	110.72	0.933	128.32	0.805

Table 5a. *V* Series Test Results with
M_s based on DSM, V_v based on AS4600 and AS4100

Test	Section	M_T (kNm)	V_T (kN)	M_{sl} (kNm)	M_{sd} (kNm)	$\dfrac{M_T}{M_{sl}}$	$\dfrac{M_T}{M_{sd}}$	V_v (AS4600) (kN)	$\dfrac{V_T}{V_{v(AS4600)}}$	V_v (AS4100) (kN)	$\dfrac{V_T}{V_{v(AS4100)}}$
MV1	C15015	10.72	35.74	9.60	8.62	1.117	1.243	27.58	1.296	43.00	0.831
MV2	C15015	10.06	33.53	9.63	8.65	1.045	1.163	27.54	1.217	43.03	0.779
MV3	C15015	10.64	35.45	9.62	7.86	1.105	1.353	27.58	1.285	43.00	0.824
MVw	C15015	8.04	26.80	9.61	7.86	0.837	1.023	27.55	0.973	43.02	0.623
MV1	C15019	14.80	49.34	14.04	11.02	1.054	1.343	56.20	0.878	67.70	0.729
MV2	C15019	14.09	46.97	14.03	11.01	1.004	1.280	56.32	0.834	67.67	0.694
MV3	C15019	14.64	48.80	13.96	10.88	1.049	1.346	56.43	0.865	67.65	0.721
MVw	C15019	11.52	38.41	14.03	10.98	0.822	1.050	56.25	0.683	67.69	0.567
MV1	C15024	19.04	63.45	16.28	14.34	1.169	1.327	91.39	0.694	96.53	0.657
MV2	C15024	19.73	65.76	16.26	14.30	1.213	1.380	91.39	0.720	96.51	0.681
MV3	C15024	18.83	62.77	16.49	14.89	1.142	1.264	91.39	0.687	96.40	0.651
MVw	C15024	16.25	54.18	16.27	14.38	0.999	1.130	91.39	0.593	96.56	0.561
MV1	C20015	13.97	34.92	12.81	10.67	1.090	1.309	20.24	1.725	46.13	0.757
MV2	C20015	12.87	32.17	12.77	10.59	1.007	1.215	20.22	1.591	46.18	0.697
MV3	C20015	14.22	35.56	12.79	10.59	1.112	1.344	20.29	1.752	46.02	0.773
MVw	C20015	9.70	24.25	12.81	10.66	0.757	0.910	20.25	1.197	46.11	0.526
MV1	C20019	22.28	55.70	19.00	15.29	1.173	1.457	41.67	1.337	67.64	0.824
MV2	C20019	21.85	54.62	18.98	15.24	1.151	1.434	41.70	1.310	67.61	0.808
MV3	C20019	21.28	53.20	18.93	15.16	1.124	1.403	41.65	1.277	67.66	0.786
MVw	C20019	15.92	39.80	18.95	15.20	0.840	1.047	41.67	0.955	67.63	0.588
MV1	C20024	29.40	73.51	26.41	21.19	1.113	1.387	83.98	0.875	102.97	0.714
MV2	C20024	28.90	72.26	26.70	21.80	1.083	1.326	84.01	0.860	102.96	0.702
MV3	C20024	28.65	71.63	26.67	21.75	1.074	1.317	84.07	0.852	102.94	0.696
MVw	C20024	22.12	55.30	26.40	21.13	0.838	1.047	83.83	0.660	103.01	0.537

Table 5b. *MV* Series Test Results with
M_s based on DSM, V_v based on AS4600 and AS4100

Test	Section	M_T (kNm)	V_T (kN)	M_{sl} (kNm)	M_{sd} (kNm)	$\dfrac{M_T}{M_{sl}}$	$\dfrac{M_T}{M_{sd}}$	V_v (AS4600) (kN)	$\dfrac{V_T}{V_{v(AS4600)}}$	V_v (AS4100) (kN)	$\dfrac{V_T}{V_{v(AS4100)}}$
M1	C15015	10.43	13.03	9.56	7.67	1.090	1.360	23.19	0.562	24.23	0.538
Mw	C15015	9.47	11.84	9.62	7.95	0.985	1.192	23.32	0.508	24.37	0.486
M1	C15019	15.86	19.82	13.97	10.95	1.135	1.448	47.38	0.418	49.51	0.400
Mw	C15019	12.94	16.18	13.90	10.86	0.931	1.192	47.43	0.341	49.56	0.326
M1	C15024	19.84	24.80	16.84	15.35	1.178	1.293	83.88	0.296	96.88	0.256
Mw	C15024	17.76	22.20	16.45	14.90	1.080	1.192	83.88	0.265	96.30	0.231
M1	C20015	13.47	16.83	12.70	10.57	1.060	1.274	17.08	0.986	17.85	0.943
Mw	C20015	12.20	15.25	12.74	10.65	0.958	1.145	17.08	0.892	17.85	0.854
M1	C20019	21.76	27.20	19.13	15.33	1.137	1.419	34.90	0.779	36.46	0.746
Mw	C20019	18.85	23.56	18.89	15.14	0.998	1.245	35.07	0.672	36.64	0.643
M1	C20024	31.39	39.24	26.98	21.98	1.163	1.428	71.17	0.551	74.36	0.528
Mw	C20024	27.88	34.86	26.90	21.91	1.037	1.273	70.77	0.493	73.95	0.471

Table 5c. *M* Series Test Results with
M_s based on DSM, V_v based on AS4600 and AS4100

As can be seen in Fig. 7a, which shows the interaction between (M_T/M_s) and (V_T/V_v) with straps where M_s is based on the EWM and V_v is based on AS 4600:2005, the interaction between bending and shear is not significant. The ratios V_T/V_v vary from 0.912 to 1.943 for the predominantly shear *(V)* and from

0.687 to 1.752 for the combined bending and shear *(MV)* test series, whereas the ratios of M_T/M_s are in the range from 0.911 to 0.983 for the *(V)* test series and from 1.079 to 1.335 for the *(MV)* test series. The explanation for this fact is that the V_v, based on AS 4600:2005, is calculated by using the elastic buckling stress of the web panel only which provides very conservative predictions, whereas the test results are based on the ultimate strength of the full section including tension field action. It is interesting to note that the slender sections (e.g. C20015 and C15015) are more conservative than stockier sections. Fig. 7b shows the comparisons for the tests without straps at the loading points. The results are lower than those in Fig. 7a but are still conservative. This situation may well occur in practice at a support point. Figs 6a and 6b show the corresponding buckling mode shapes of the C-section members with and without straps respectively for the *MV* test series.

(a) With Straps   (b) Without Straps

Figure 6. Buckling Mode Shape of C-Section Members

Fig. 8a shows the interaction between (M_T/M_s) and (V_T/V_v) with straps where M_s is based on the EWM and V_v is based on AS4100-1998. The ratios V_T/V_v are in the range 0.827 to 0.993 and 0.651 to 0.831 for *V* and *MV* test series respectively, whereas the ratios of M_T/M_s are the same as those in Fig. 7a. This method, therefore, gives more accurate prediction on the postbuckling strengths of web elements for bending and shear. The two vertical rows of bolts have increased the restraints to the web panel and act as web stiffeners. These increased restraints have improved the postbuckling strengths of the web for the *(V)* and the *(MV)* test series. Further, with the *V* and *MV* test series, the ratios of shear span *(s)* to depth *(d₁)* are 1:1 and 2:1 respectively which enabled the formation of diagonal tension field action. Although the postbuckling strength factor for shear is utilized for steel member when the web is provided with intermediate transverse stiffeners according to AS 4100-1998, it is also applicable to the cold-formed lipped channel sections in this investigation. It can be seen in Fig. 8b which shows the interaction between (M_T/M_s) and (V_T/V_v) without straps where M_s is based on the EWM and V_v is based on AS4100-1998, the interaction between bending and shear is significant especially for the *(MV)*

test series. The results are lower than those in Fig. 7b and lie below Eq. 2 trilinear. This fact shows that the existing Eq. 2 for design is unconservative especially for the combined bending and shear without straps when considering the effect of tension field action. It is believed that the straps may assist tension field action.

Fig. 9a shows the interaction between (M_T/M_s) and (V_T/V_v) with straps where M_s is based on the DSM and V_v is based on AS 4600:2005. In this figure, M_s is determined by using nominal section moment capacity at local buckling (M_{sl}) only. While the ratios of V_T/V_v are the same as those in Fig. 7a, the ratios of M_T/M_s vary from 0.819 to 0.918 for the (V) test series and from 1.004 to 1.213 for (MV) test series. The interaction bending and shear is not significant. The explanation for this fact is quite similar to that in Fig. 7a. It is interesting to note that the nominal section moment capacities predicted by the DSM are more accurate and less variable than those predicted by the EWM. As can be also seen in Fig. 9b which shows interaction between (M_T/M_s) and (V_T/V_v) without straps where M_s is based on the DSM and V_v is based on AS 4600:2005, the results are lower and are mainly conservative except C15019 and C20024 (MV) tests which lie below Eq.2 trilinear. In Fig. 10, the interaction between (M_T/M_s) and (V_T/V_v) without straps is similar to that in Fig. 9b. The only difference is that the nominal section moment capacity at distortional buckling (M_{sd}) is utilized instead of M_{sl}. The results are shifted up higher than those in Fig. 9b and lie above Eq. 2 trilinear. The interaction is therefore not significant and very conservative.

Fig. 11a shows the interaction between (M_T/M_s) and (V_T/V_v) with straps where M_s is based on the DSM and V_v is based on AS4100-1998 with tension field action. In this figure, M_s is determined by using nominal section moment capacity at local buckling (M_{sl}) only. Because of the presence of the straps screwed on top flanges adjacent to loading point and reactions, the channel section are enforced to fail in local buckling. By comparison of values with Fig. 8a where M_s is based on the EWM, for bending, the ratios M_T/M_s for the (V) test series of both methods are slightly different and in the range 0.911 to 0.983 for the EWM and 0.800 to 0.907 for the DSM. For (MV) test series, the ratios M_T/M_s are from 1.079 to 1.335 for the EWM and from 1.004 to 1.213 for the DSM. For (M) test series, the EMW range is from 1.132 to 1.346 and the DSM range is from 1.060 to 1.178. The EMW is generally less accurate and more variable than the DSM.

Fig. 11b shows the interaction between (M_T/M_s) and (V_T/V_v) without straps where M_s is based on M_{sl} and V_v is based on AS4100-1998 with tension field action. It can be seen in this figure that the interaction between bending and shear is very significant. Most tests for (MV) test series lie below Eq. 2 trilinear and are closer to Eq. 1 unit circle. Some tests for (V) test series are also below

Eq. 2 trilinear. This fact shows that it is unconservative to use Eq. 2 trilinear for design with M_{sl} and tension field action included and the Eq. 1 unit circle may be applicable in this case. In Fig. 12, the nominal section moment capacity at distortional buckling (M_{sd}) is utilized instead of M_{sl}. The results are higher than those in Fig. 11b and generally lie above Eq. 2 trilinear. The interaction is therefore not significant and conservative. The explanation is due to the fact that M_{sd} is normally lower than M_{sl} and it is conservative to use M_{sd} to predict M_s in the case of tests without straps.

(a) With Straps	(b) Without Straps
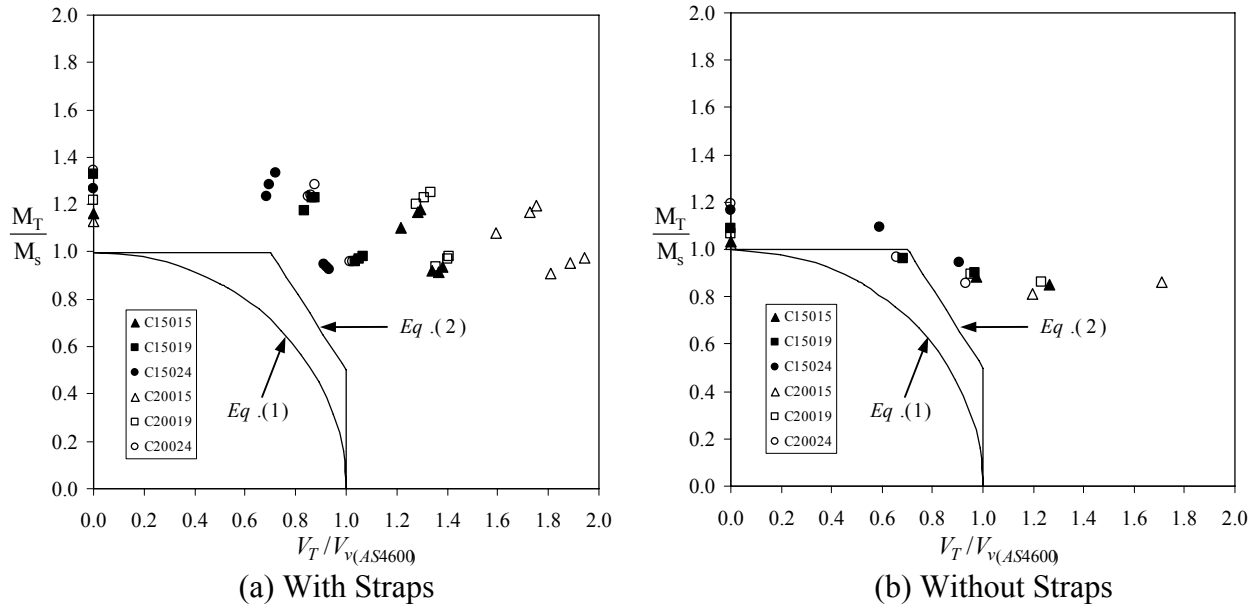
Figure 7. Interaction between (M_T/M_s) and (V_T/V_v) with M_s based on EWM, V_v based on AS4600

(a) With Straps	(b) Without Straps
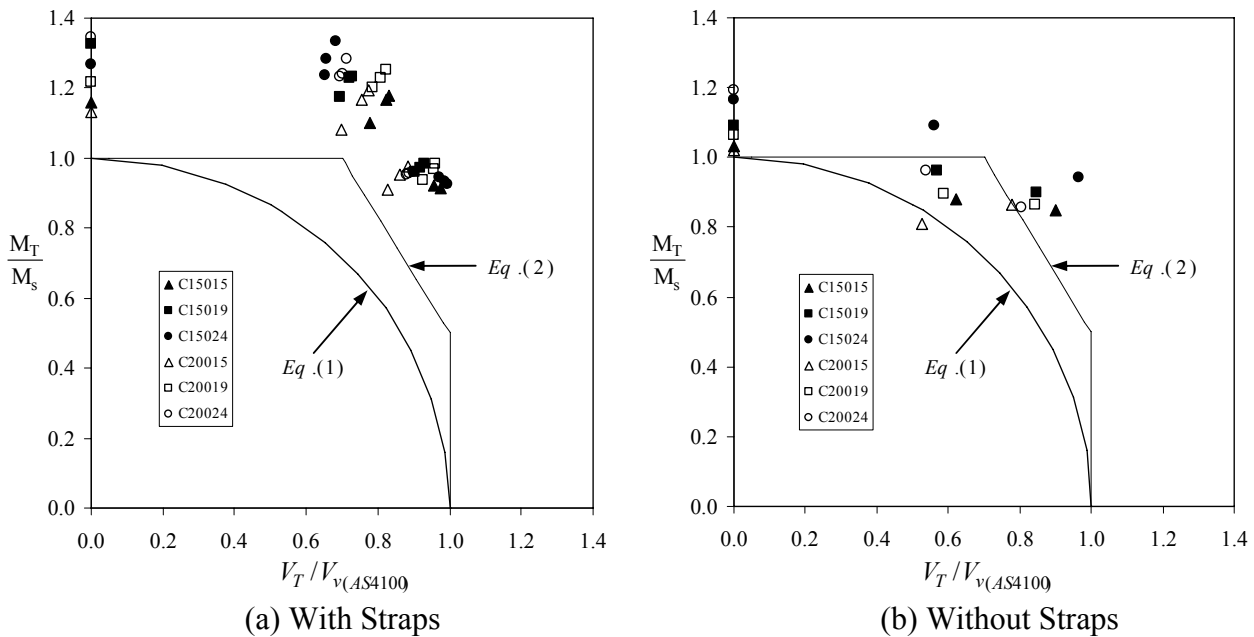
Figure 8. Interaction between (M_T/M_s) and (V_T/V_v) with M_s based on EWM, V_v based on AS4100

(a) With Straps
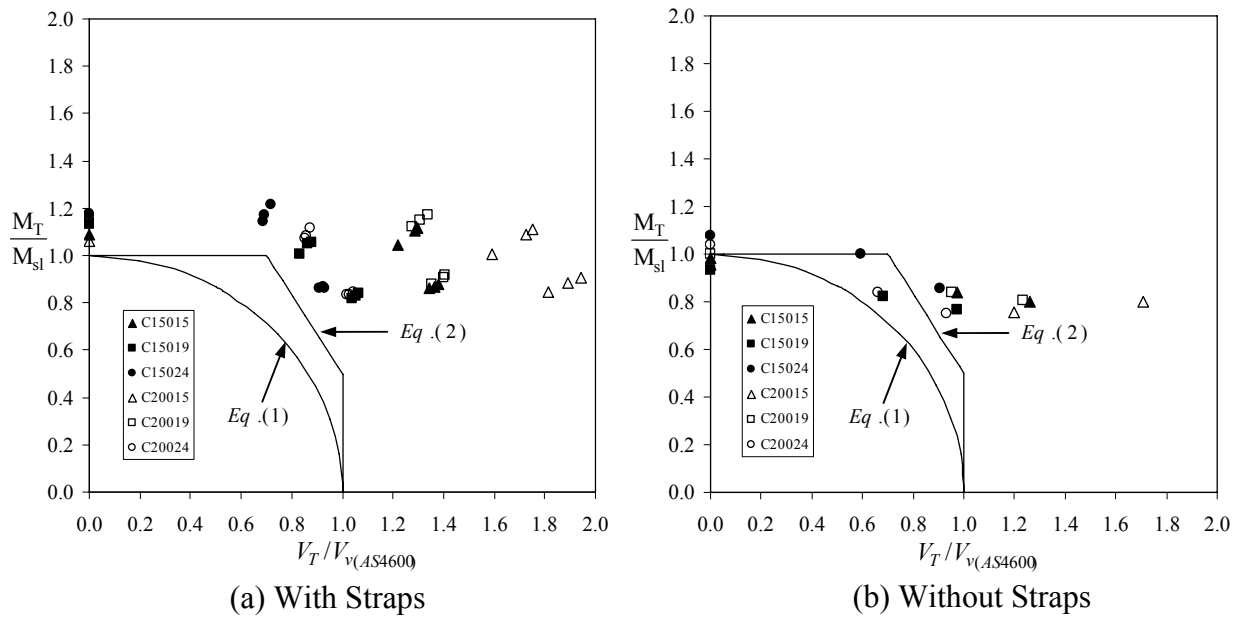
(b) Without Straps

Figure 9. Interaction between (M_T/M_s) and (V_T/V_v) with M_{sl} based on DSM, V_v based on AS4600
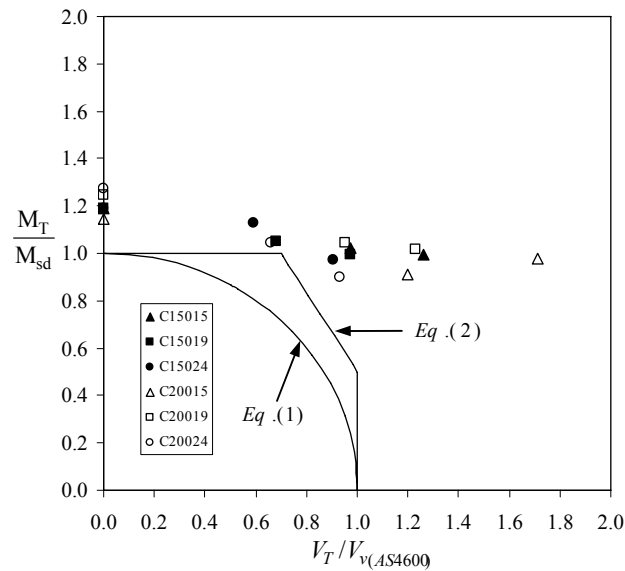
Figure 10. Interaction between (M_T/M_s) and (V_T/V_v) with M_{sd} based on DSM, V_v based on AS4600 – without straps

(a) With Straps   (b) Without Straps
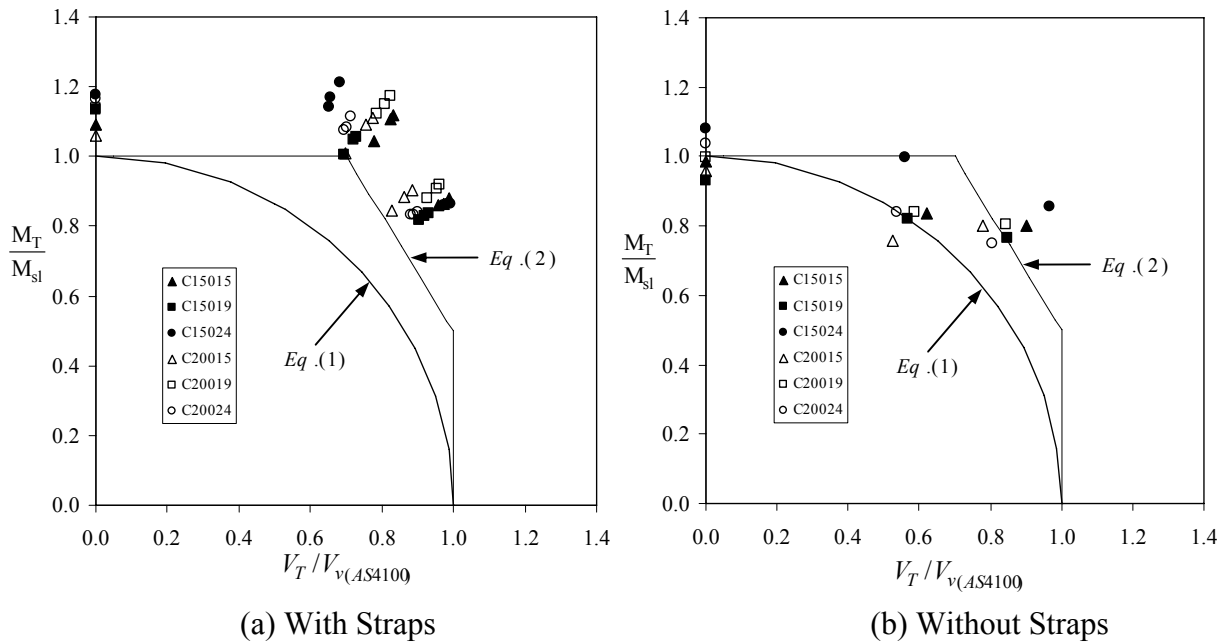
Figure 11. Interaction between (M_T/M_s) and (V_T/V_v) with M_{sl} based on DSM, V_v based on AS4100
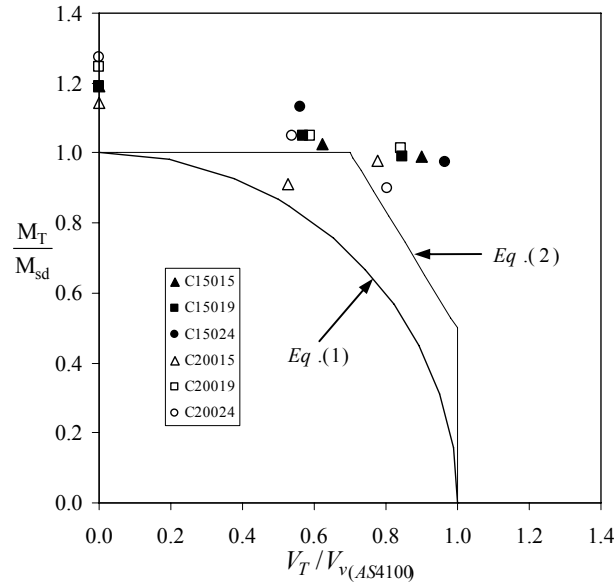
Figure 12. Interaction between (M_T/M_s) and (V_T/V_v)
with M_{sd} based on DSM, V_v based on AS4100 – without straps

6 DESIGN PROPOSALS

For EWM:

When the Clause 3.3.4.1 of AS 4600:2005 was used to predict the shear capacity without tension field action, the proposed interaction equation in Clause 3.3.5 for combined bending and shear of AS 4600:2005 could be Eq. 2 trilinear both with and without straps (see Figs. 7a and 7b). When stiffening occurs at the loading points, Eq. 2 trilinear is confirmed for the EWM, both with and without the straps.

When the Clause 5.11.2 of AS 4100-1998 was used to predict the shear capacity accounting for tension field action, the proposed interaction equation in Clause 3.3.5 for combined bending and shear of AS 4600:2005 could be Eq. 2 trilinear with straps (see Fig. 8a) and must be Eq. 1 circular curve without straps (see Fig. 8b). A tension field action clause could be added to AS/NZS 4600 in the EWM. However, the lower interaction equation (Eq. 1) curve would need to be used.

For DSM:

Clause 7.2.2.5 of AS 4600:2005 for pure shear is proposed based on Clause 3.3.4.1 of AS 4600:2005 in DSM format to predict the shear capacity without tension field action. The proposed interaction equation in Clause 7.2.2.6 for combined bending and shear of AS 4600:2005 is Eq. 2 trilinear for M_s based on M_{sl} with straps (see Fig. 9a) and M_{sd} without straps (see Fig. 10). If M_s is based on M_{sl} without straps, the proposed interaction is Eq. 1 circular curve (see Fig. 9b). As for the EWM, the existing Eq. 1 interaction curve could be replaced by Eq. 2 trilinear if M_s is based on M_{sd} in the DSM.

If Clause 7.2.2.5 of AS 4600:2005 for pure shear is based on Clause 5.11.2 of AS 4100-1998 to predict the shear capacity with tension field action, the proposed interaction Clause 7.2.2.6 for combined bending and shear of AS 4600:2005 is Eq. 2 trilinear for M_s based on M_{sl} with straps (see Fig. 11a) and M_{sd} without straps (see Fig. 12). If M_s is based on M_{sl} without straps, the proposed interaction is Eq. 1 circular curve (see Fig.11b). A tension field action clause could be added to AS/NZS 4600 in the DSM. However, the lower interaction equation (Eq. 1) would need to be used if M_s was based on M_{sl} and not M_{sd}.

7 CONCLUSION

An experimental program was carried out to determine the ultimate strength of high strength cold-formed channel sections subjected to predominantly shear, combined bending and shear, and bending only. A total of 60 tests of two different depths and three different thicknesses have been performed in the above series. While 42 tests were conducted with straps at the loading points, the remaining 18 tests were tested without straps. The test results are plotted in this report as interaction diagrams where V_v and M_s are determined by different methods. The shear capacity, V_v, is based on both AS 4600:2005 and AS 4100-1998 accounting for tension field action. The nominal section moment capacity, M_s, is based on both the EWM and DSM.

The tests confirm that the current EWM satisfies Eq. 2 trilinear interaction even for tests without straps. The tests show that the DSM requires $M_s=M_{sd}$ to satisfy Eq. 2 trilinear interaction. Also if tension field action is included, then Eq. 1 circular interaction must be used with $M_s=M_{sl}$ but Eq. 2 trilinear interaction can be used with $M_s=M_{sd}$. Tension field action cannot be used with the EWM as currently constructed but can be used with the DSM with $M_s=M_{sd}$.

ACKNOWLEDGEMENTS

NOTATION

The following symbols are used in this paper:

A_w =   Area of web (mm^2)
E =   Young's modulus (GPa)
d_1 =   Depth of the flat portion of the web measured along the plane of the web (mm)
k_v =   Shear buckling coefficient
f_{od} =   Elastic distortional buckling stress of the section in bending (MPa)
f_{ol} =   Elastic local buckling stress of the section in bending (MPa)
f_y =   Yield stress (MPa)
M_{od} =   Elastic distortional buckling moment of the section (kNm)
M_{ol} =   Elastic local buckling moment of the section (kNm)
M_{sd} =   Nominal section moment capacity at distortional buckling (kNm)
M_{sl} =   Nominal section moment capacity at local buckling (kNm)

M_y = Moment causing initial yield at the extreme compression fibre of full section (kNm)

s = spacing of stiffeners (mm)

t_w = Thickness of web (mm)

V_v = Nominal shear capacity of web (kN)

V_{cr} = Elastic shear buckling force of web (kN)

V_y = Yield load of web (kN)

Z_e = Section modulus about a horizontal axis of the effective section.

Z_f = Section modulus about a horizontal axis of the full section.

REFERENCES

American Iron and Steel Institute (AISI). (2007). "North American Specification for the Design of Cold-Formed Steel Structural Members." *AISI S100-2007*, 2007 Ed.

LaBoube, R. A., and Yu, W. W. (1978). "Cold-Formed Steel Web Elements under Combined Bending and Shear." *Proc., 4th Int. Specialty Conf. on Cold-Formed Steel Structures*, University of Missouri-Rolla, St Louis, Missouri, U.S.A.

Lau, S. C. W. and Hancock, G. J. (1986). "Buckling of Thin Flat-Walled Structures by a Spline Finite Strip Method." *Thin-Walled Structures*, Vol. 4, pp 269-294.

Pham, C. H., and Hancock, G. J. (2009a). "Shear Buckling of Thin-Walled Channel Sections" *Journal of Constructional Steel Research*, Vol 65, No 3, pp. 578-585.

Pham, C. H., and Hancock, G. J. (2009b). "Direct Strength Design of Cold-Formed Purlins." *Journal of Structural Engineering*, American Society of Civil Engineers, Vol 135, Issue 3, pp. 229-238.

Standards Australia. (1991). "Methods for Tensile Testing of Metals." *AS/NZS 1391*, Standards Australia/ Standards New Zealand.

Standards Australia. (1998). "Steel Structures." *AS/NZS 4100:1998*, Standards Australia/ Standards New Zealand.

Standards Australia (2006). "Cold-Formed Steel Structures." *AS/NZS 4600:2005*, Standards Australia/ Standards New Zealand.

Timoshenko, S. P. and Gere, J. M. (1961) "Theory of Elastic Stability." *McGraw-Hill Book Co. Inc*, New York, N.Y.

APPENDICES

Test	Section	V_y (kN)	V_{cr} (kN)	λ_v	f_{ol} (MPa)	f_{od} (MPa)	Z_e (mm³)	Z_f (mm³)	M_{ol} (kNm)	M_{od} (kNm)	M_y (kNm)	λ_l	λ_d
V1	C15015	72.93	40.59	1.340	477.5	351.0	16790	21780	10.40	7.64	11.79	1.065	1.242
V2	C15015	72.81	40.66	1.338	480.0	344.4	16640	21620	10.38	7.45	11.70	1.062	1.253
V3	C15015	72.92	40.59	1.340	480.4	325.5	16380	21460	10.31	6.99	11.61	1.061	1.289
Vw	C15015	72.84	40.64	1.339	479.6	348.5	16720	21690	10.40	7.56	11.74	1.062	1.246
V1	C15019	90.66	83.02	1.045	756.9	459.8	22180	27340	20.69	12.57	14.61	0.840	1.078
V2	C15019	90.74	82.95	1.046	761.1	460.3	22120	27220	20.72	12.53	14.55	0.838	1.078
V3	C15019	90.61	83.06	1.044	752.8	459.5	22230	27440	20.66	12.61	14.67	0.843	1.079
Vw	C15019	90.51	83.16	1.043	754.6	453.3	22100	27310	20.61	12.38	14.60	0.842	1.086
V1	C15024	103.31	168.39	0.783	1241	694.7	30750	33800	41.95	23.48	16.40	0.625	0.836
V2	C15024	103.18	168.61	0.782	1236	767.6	32010	34420	42.54	26.42	16.70	0.627	0.795
V3	C15024	103.38	168.28	0.784	1245	751.1	31620	34120	42.48	25.63	16.56	0.624	0.804
Vw	C15024	103.06	168.81	0.781	1242	689.5	30590	33690	41.84	23.23	16.35	0.625	0.839
V1	C20015	94.49	29.72	1.783	289.2	233.0	23000	35410	10.24	8.25	18.18	1.332	1.484
V2	C20015	94.41	29.75	1.781	288.6	232.9	23050	35550	10.26	8.28	18.25	1.334	1.485
V3	C20015	94.46	29.73	1.783	288.4	232.2	23030	35540	10.25	8.25	18.25	1.334	1.487
Vw	C20015	94.52	29.71	1.784	289.3	231.8	22950	35360	10.23	8.20	18.15	1.332	1.488
V1	C20019	116.96	61.46	1.380	462.6	319.7	34470	44860	20.75	14.34	22.90	1.050	1.264
V2	C20019	116.97	61.45	1.380	461.0	329.3	34860	45250	20.86	14.90	23.10	1.052	1.245
V3	C20019	116.78	61.55	1.377	461.6	328.3	34780	45170	20.85	14.83	23.06	1.052	1.247
Vw	C20019	116.80	61.54	1.378	463.3	319.7	34410	44770	20.74	14.31	22.85	1.050	1.264
V1	C20024	140.47	123.39	1.067	735.0	539.7	49590	58270	42.83	31.45	28.17	0.811	0.946
V2	C20024	140.02	123.78	1.064	735.9	522.8	49030	57940	42.64	30.29	28.01	0.811	0.962
V3	C20024	139.65	124.11	1.061	743.3	529.0	48710	57380	42.65	30.35	27.74	0.807	0.956
Vw	C20024	140.60	123.28	1.068	732.0	542.0	49870	58590	42.89	31.76	28.33	0.813	0.944

Appendix 1: *V* Series Test Design Criteria based on the DSM

Test	Section	V_y (kN)	V_{cr} (kN)	λ_v	f_{ol} (MPa)	f_{od} (MPa)	Z_e (mm³)	Z_f (mm³)	M_{ol} (kNm)	M_{od} (kNm)	M_y (kNm)	λ_l	λ_d
MV1	C15015	72.86	27.58	1.625	482.1	460.3	16840	21680	10.45	9.98	11.73	1.059	1.084
MV2	C15015	72.96	27.54	1.628	478.5	457.1	16870	21800	10.43	9.96	11.80	1.063	1.088
MV3	C15015	72.85	27.58	1.625	477.3	355.5	16850	21810	10.41	7.75	11.80	1.065	1.234
MVw	C15015	72.93	27.55	1.627	480.6	358.7	16850	21720	10.44	7.79	11.75	1.061	1.228
MV1	C15019	90.90	56.20	1.272	747.2	468.4	22490	27730	20.72	12.99	14.82	0.846	1.068
MV2	C15019	90.72	56.32	1.269	745.8	467.8	22470	27730	20.68	12.97	14.82	0.847	1.069
MV3	C15019	90.54	56.43	1.267	747.9	459.9	22300	27570	20.62	12.68	14.74	0.845	1.078
MVw	C15019	90.82	56.25	1.271	745.0	463.7	22450	27730	20.66	12.86	14.82	0.847	1.074
MV1	C15024	102.96	114.69	0.947	1249.0	693.3	30530	33550	41.90	23.26	16.28	0.623	0.837
MV2	C15024	102.94	114.72	0.947	1249.0	689.6	30460	33500	41.84	23.10	16.26	0.623	0.839
MV3	C15024	102.83	114.84	0.946	1248.0	749.9	31420	33980	42.41	25.48	16.49	0.624	0.804
MVw	C15024	103.00	114.65	0.948	1252.0	699.8	30590	33530	41.98	23.46	16.27	0.623	0.833
MV1	C20015	94.17	20.24	2.157	289.5	242.8	23330	35620	10.31	8.65	18.29	1.332	1.454
MV2	C20015	94.26	20.22	2.159	289.7	239.8	23220	35520	10.29	8.52	18.24	1.331	1.463
MV3	C20015	93.94	20.29	2.151	289.7	239.1	23190	35550	10.30	8.50	18.25	1.331	1.465
MVw	C20015	94.12	20.25	2.156	289.3	241.8	23310	35640	10.31	8.62	18.30	1.332	1.457
MV1	C20019	117.10	41.67	1.676	460.1	328.8	34890	45320	20.85	14.90	23.13	1.053	1.246
MV2	C20019	117.02	41.70	1.675	460.0	326.6	34820	45280	20.83	14.79	23.11	1.053	1.250
MV3	C20019	117.15	41.65	1.677	461.1	325.5	34730	45130	20.81	14.69	23.04	1.052	1.252
MVw	C20019	117.08	41.67	1.676	460.8	326.4	34770	45190	20.82	14.75	23.07	1.053	1.251
MV1	C20024	140.11	83.98	1.292	750.4	493.5	47420	55790	41.86	27.53	26.97	0.803	0.990
MV2	C20024	140.05	84.01	1.291	749.4	517.4	48130	56430	42.29	29.20	27.28	0.803	0.967
MV3	C20024	139.94	84.07	1.290	750.2	516.1	48040	56350	42.27	29.08	27.24	0.803	0.968
MVw	C20024	140.34	83.83	1.294	748.4	488.6	47410	55810	41.77	27.27	26.98	0.804	0.995

Appendix 2: *MV* Series Test Design Criteria based on the DSM

Test	Section	V_y (kN)	V_{cr} (kN)	λ_v	f_{ol} (MPa)	f_{od} (MPa)	Z_e (mm³)	Z_f (mm³)	M_{ol} (kNm)	M_{od} (kNm)	M_y (kNm)	λ_l	λ_d
M1	C15015	72.97	23.194	1.774	479.3	340.3	16610	21640	10.37	7.36	11.71	1.063	1.261
Mw	C15015	72.57	23.320	1.764	479.6	367.5	16930	21770	10.44	8.00	11.78	1.062	1.213
M1	C15019	90.82	47.379	1.385	755.7	471.7	22370	27500	20.78	12.97	14.70	0.841	1.064
Mw	C15019	90.72	47.434	1.383	763.5	471.5	22220	27260	20.81	12.85	14.57	0.837	1.065
M1	C15024	103.34	96.255	1.036	1226.0	772.0	32280	34700	42.54	26.79	16.84	0.629	0.793
Mw	C15024	102.72	96.835	1.030	1252.0	757.2	31450	33900	42.44	25.67	16.45	0.623	0.801
M1	C20015	94.01	17.080	2.346	292.1	243.8	23170	35220	10.29	8.59	18.08	1.326	1.451
Mw	C20015	93.99	17.083	2.346	291.8	246.3	23280	35330	10.31	8.70	18.14	1.326	1.444
M1	C20019	117.77	34.896	1.837	454.1	321.6	35000	45830	20.81	14.74	23.40	1.060	1.260
Mw	C20019	117.20	35.068	1.828	462.7	326.8	34700	44980	20.81	14.70	22.96	1.050	1.250
M1	C20024	139.24	71.167	1.399	741.9	509.6	48240	57200	42.44	29.15	27.66	0.807	0.974
Mw	C20024	140.02	70.771	1.407	742.9	509.9	48290	57010	42.35	29.07	27.56	0.807	0.974

Appendix 3: *M* Series Test Design Criteria based on the DSM
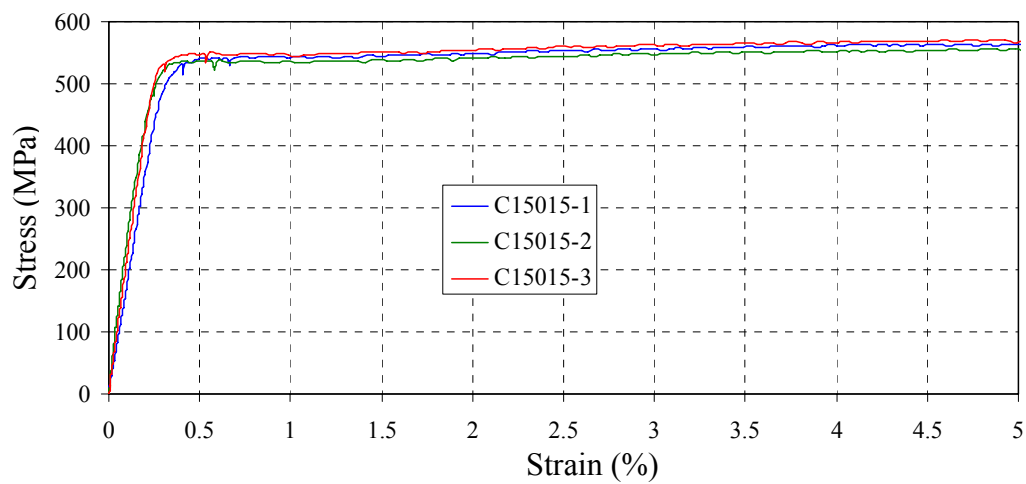
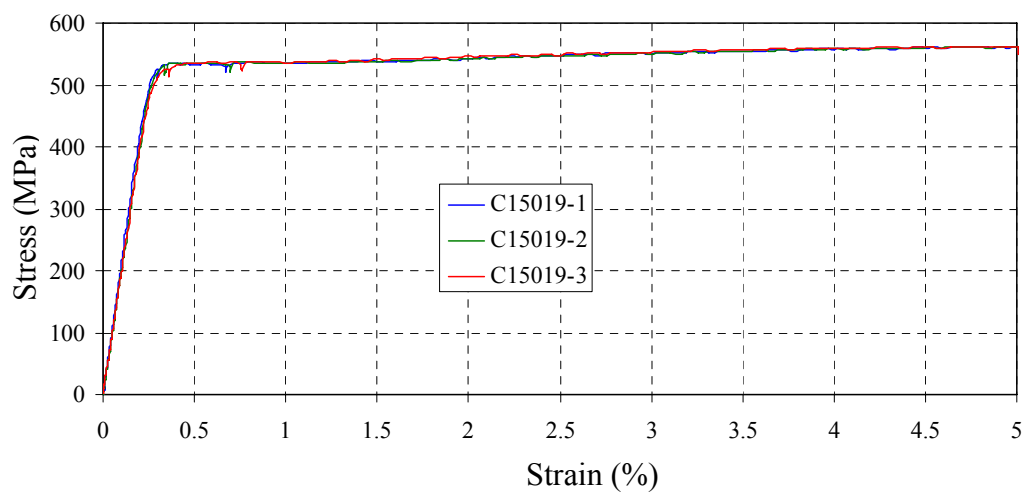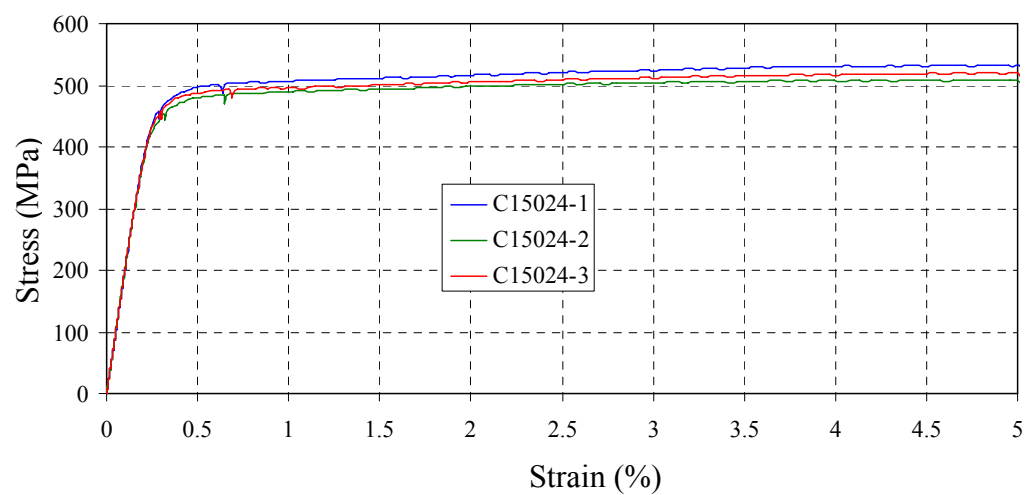Figure 13. C15015 Coupon Tests
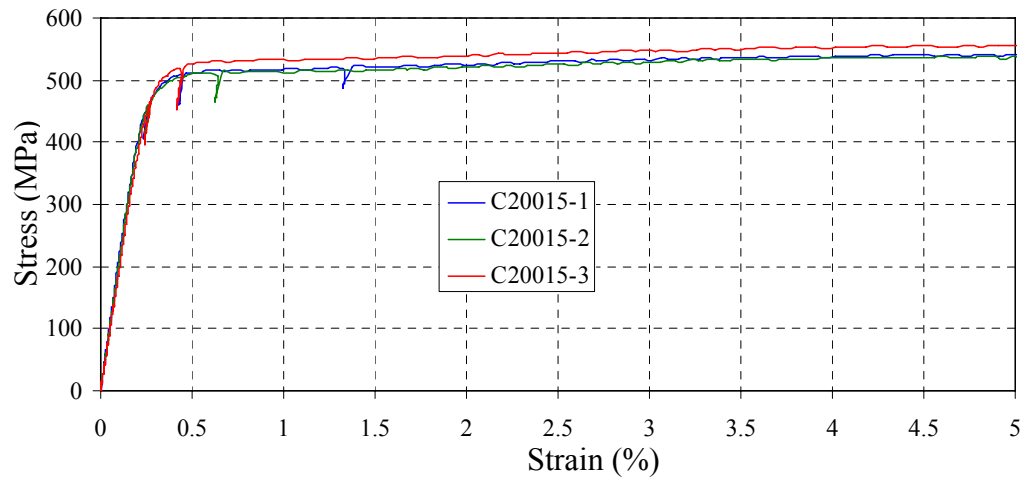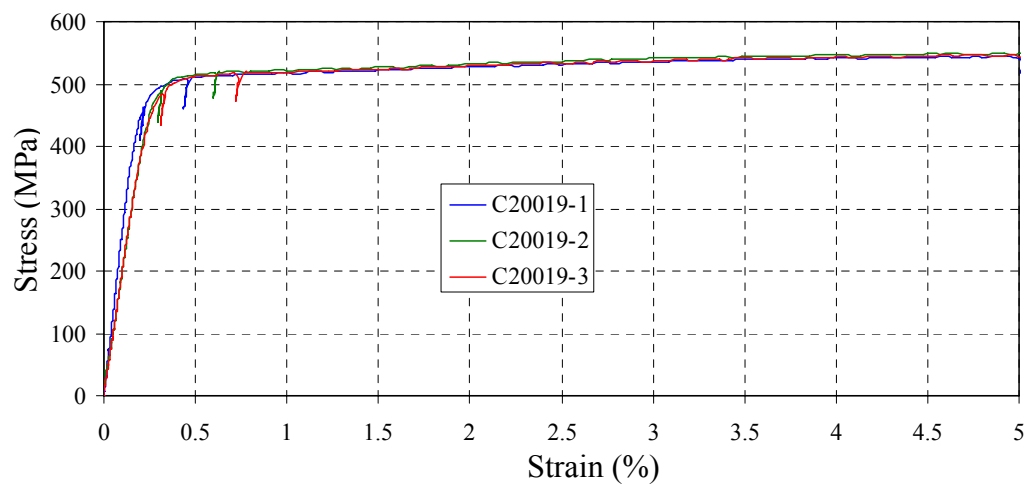

Figure 14. C15019 Coupon Tests

Figure 15. C15024 Coupon Tests

Figure 16. C20015 Coupon Tests
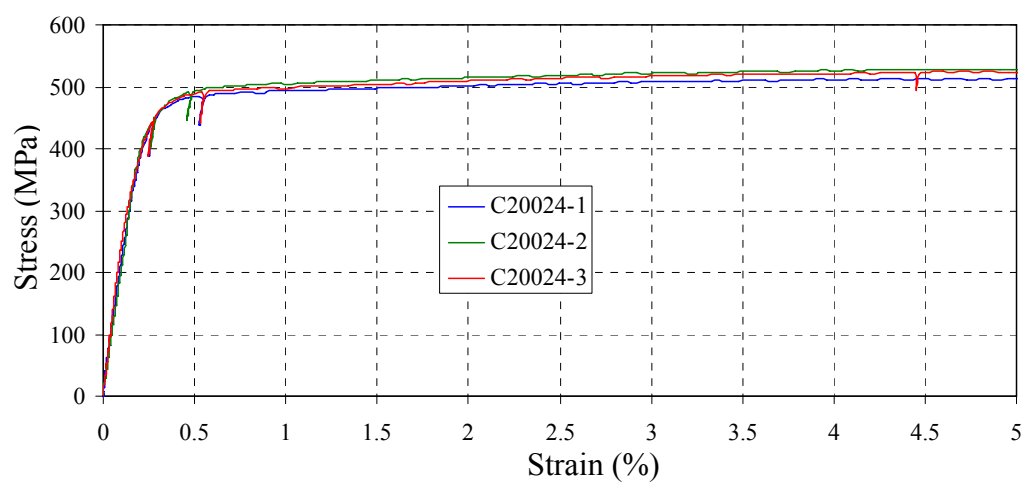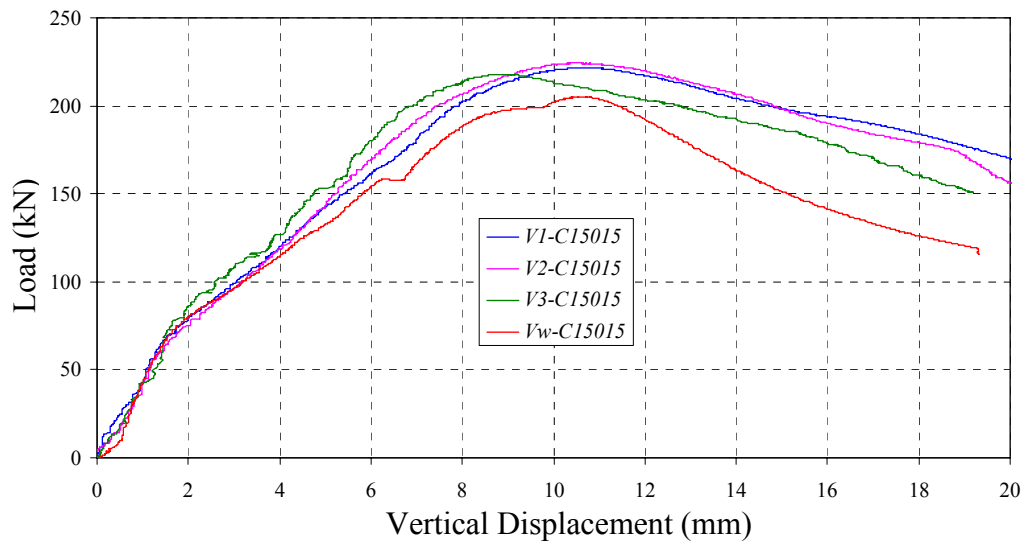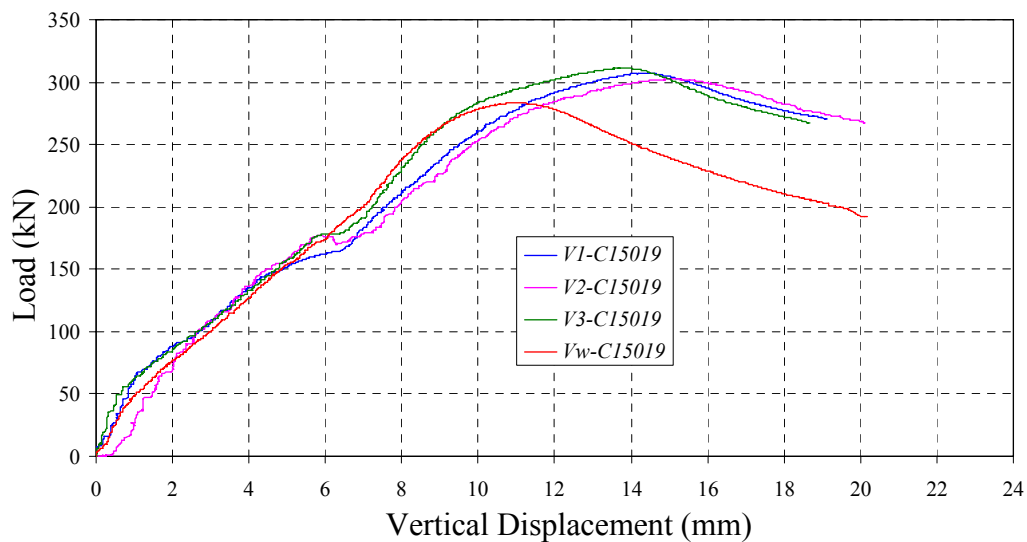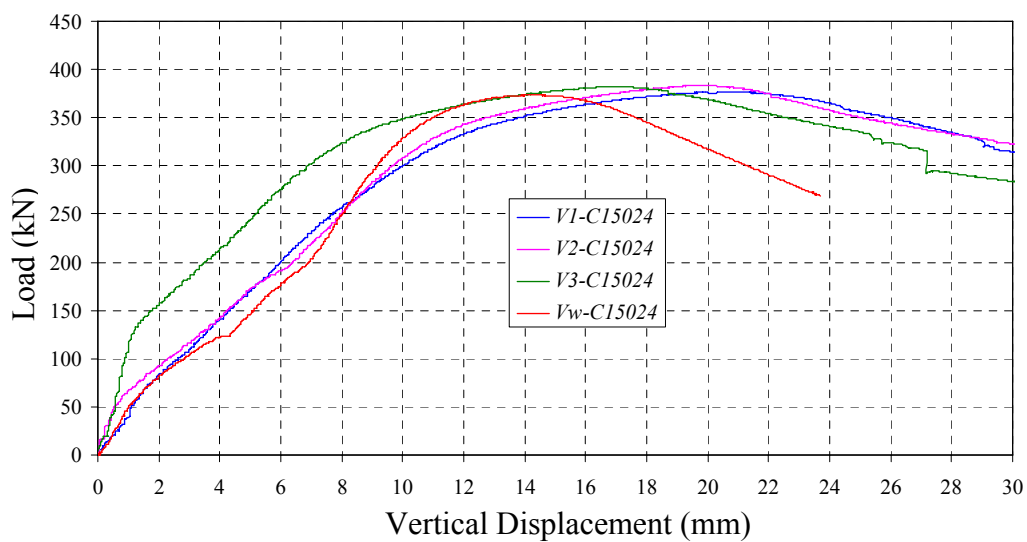

Figure 17. C20019 Coupon Tests

Figure 18. C20024 Coupon Tests

Figure 19. Load vs. Displacement-C15015-*V* Test Series

Figure 20. Load vs. Displacement-C15019-*V* Test Series

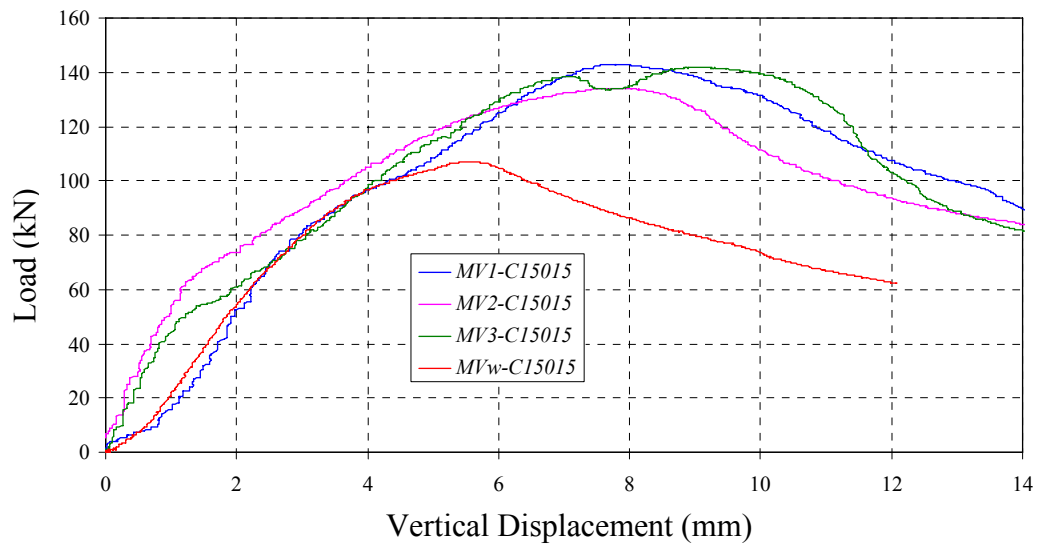Figure 21. Load vs. Displacement-C15024-*V* Test Series

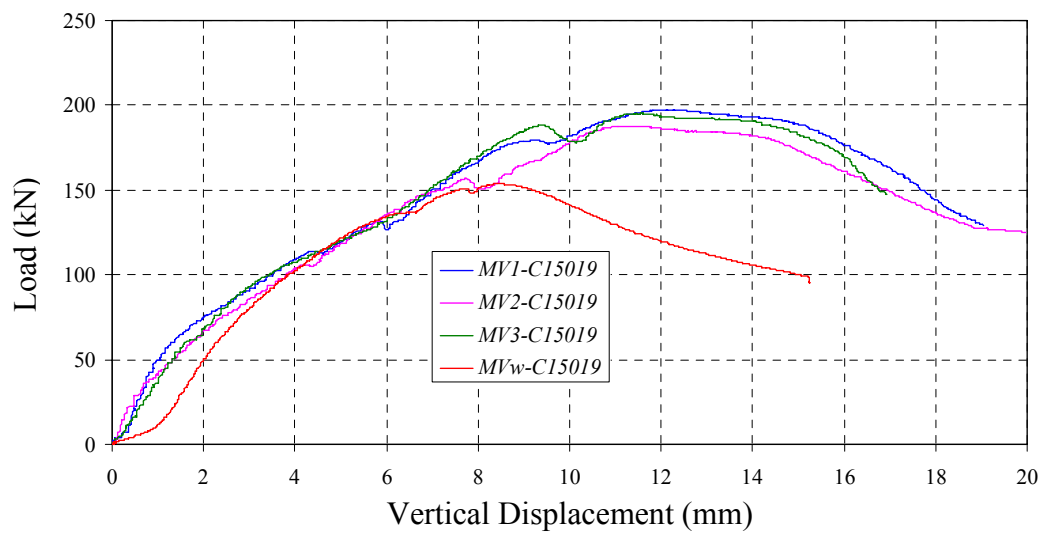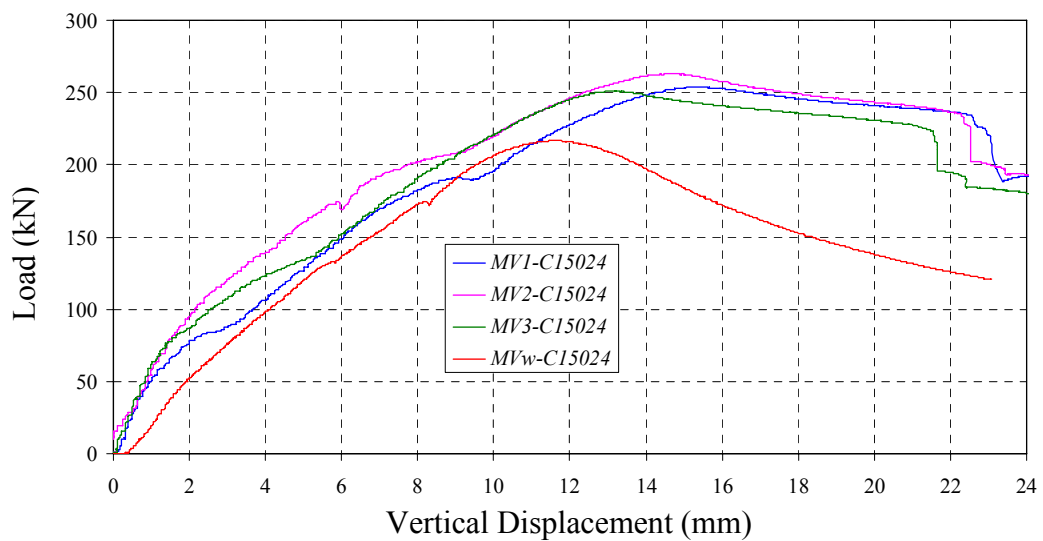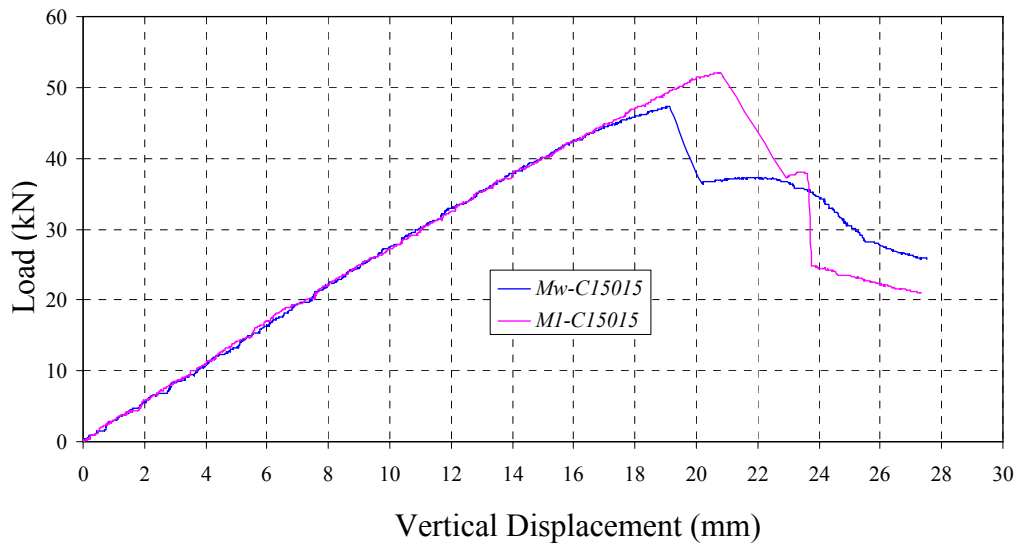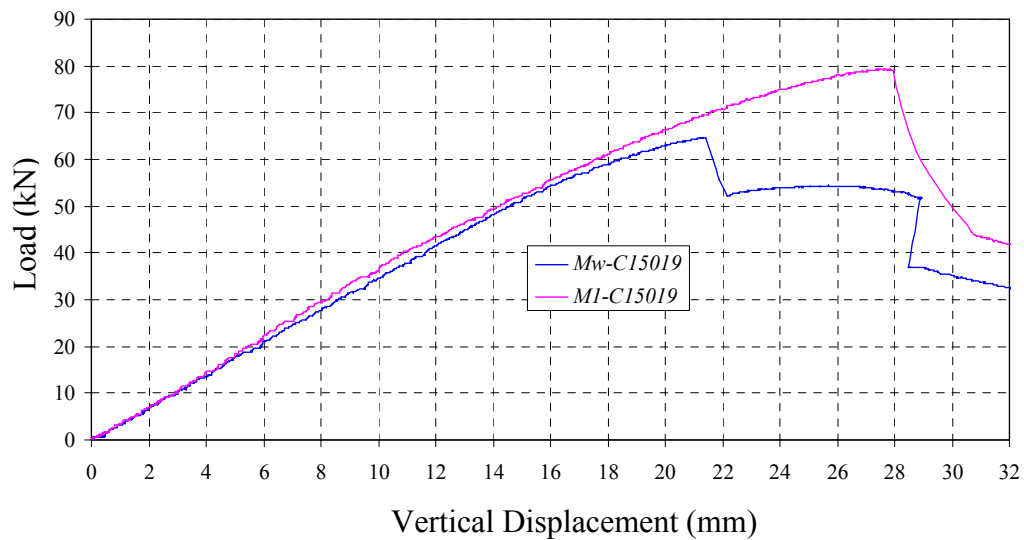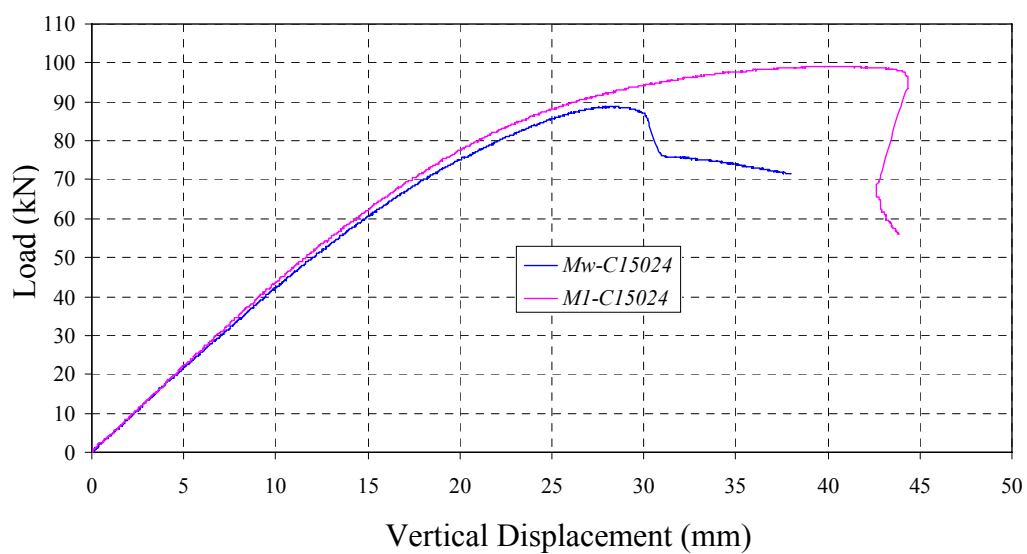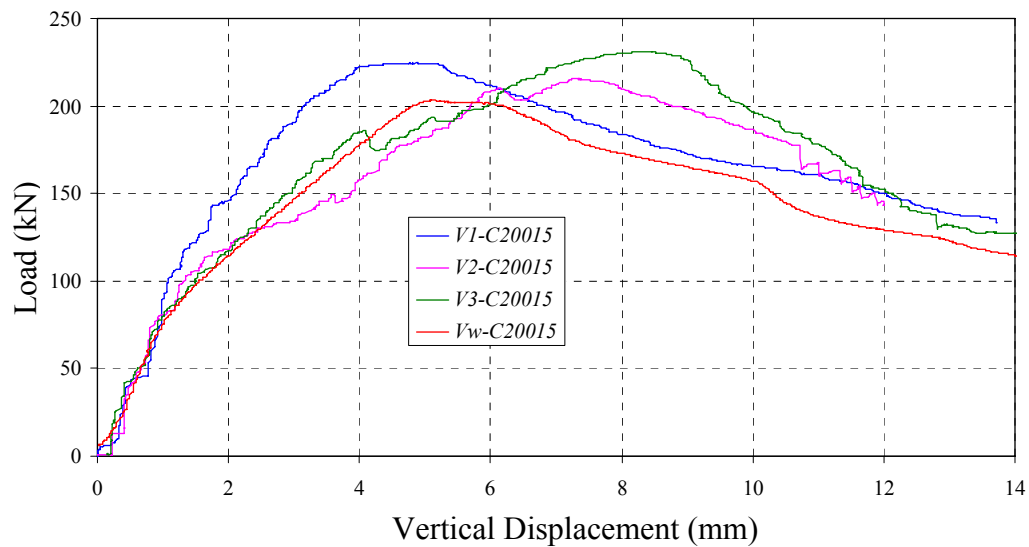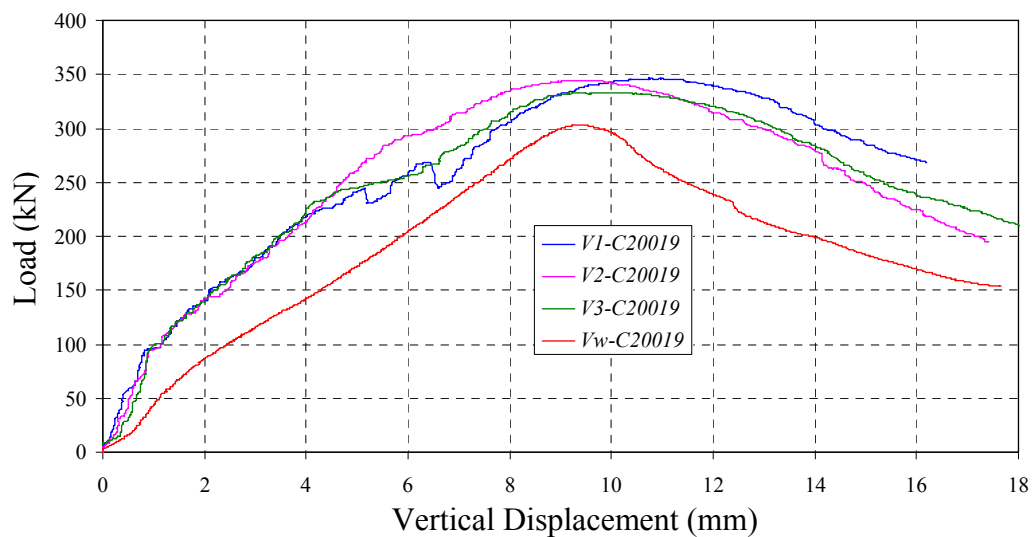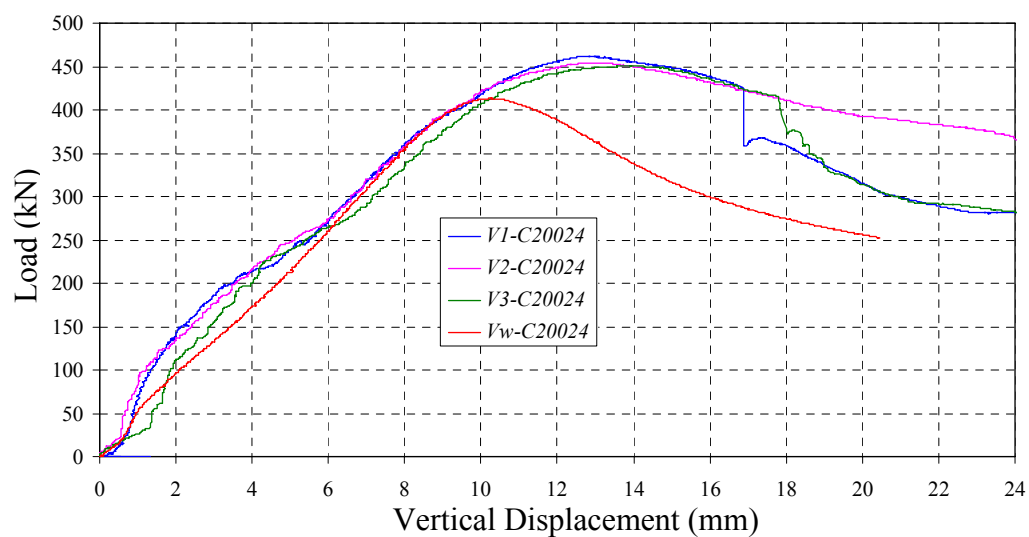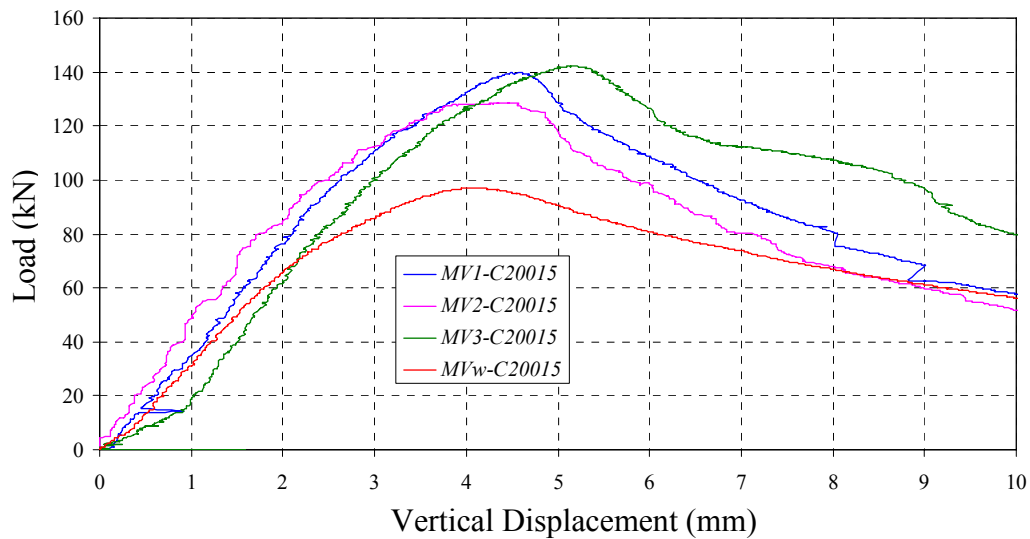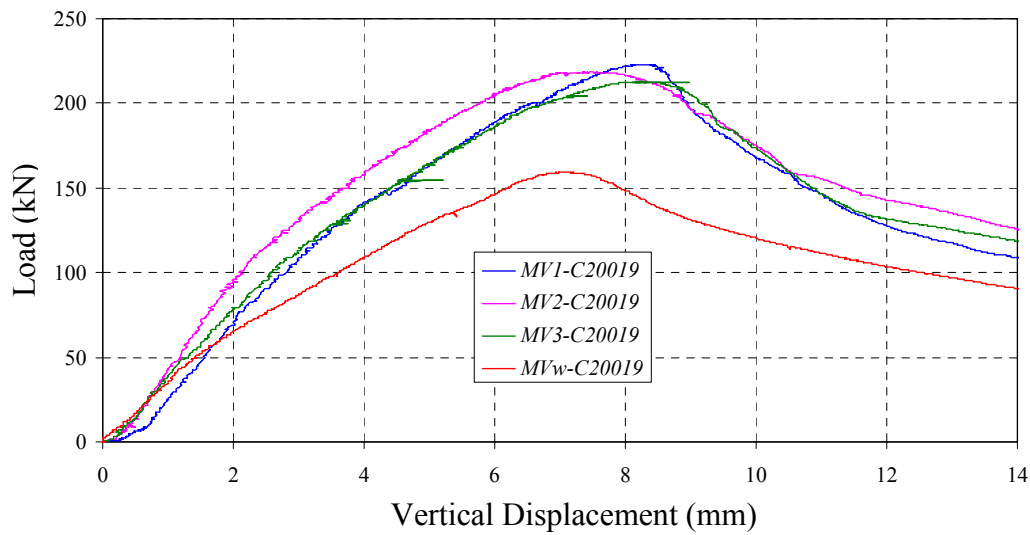Figure 22. Load vs. Displacement-C15015-*MV* Test Series

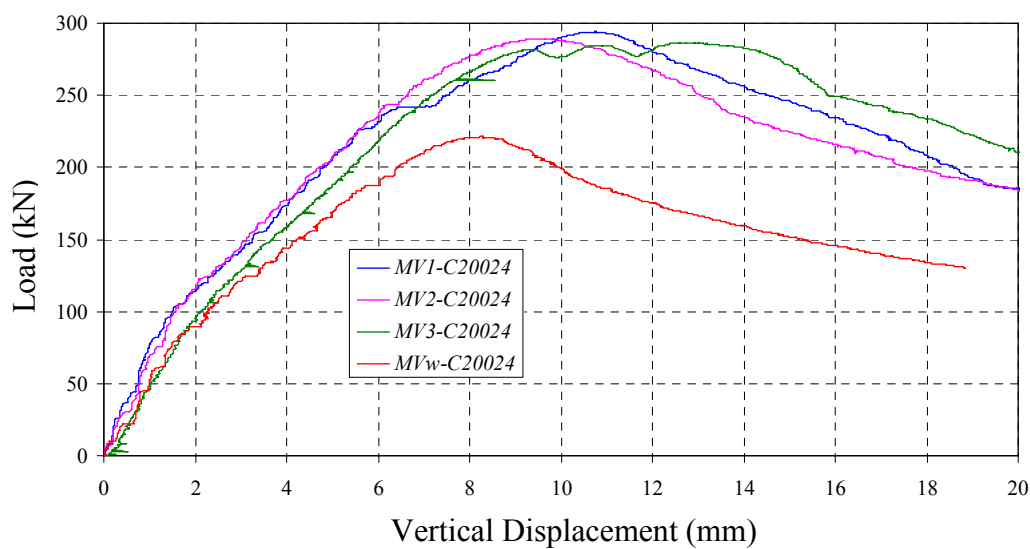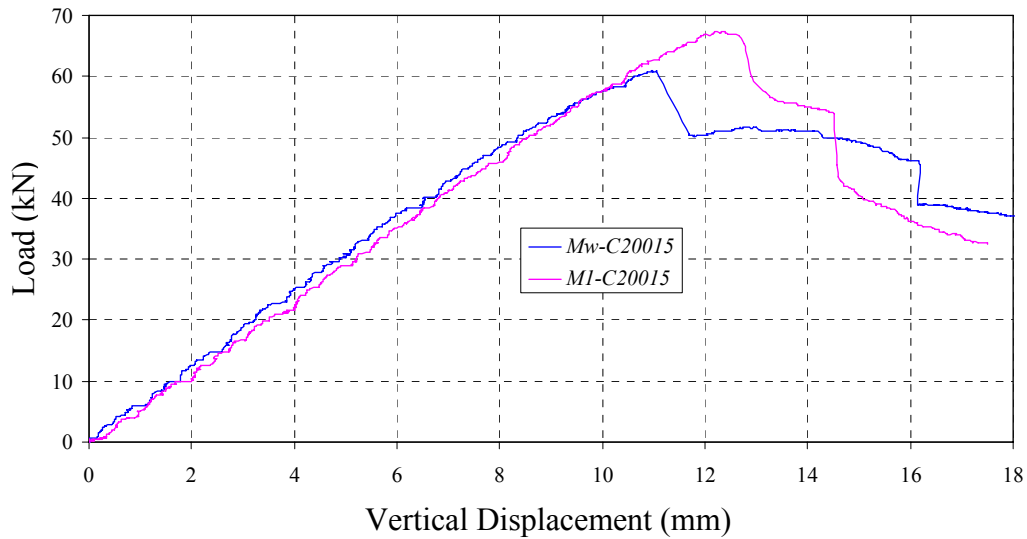Figure 23. Load vs. Displacement-C15019-*MV* Test Series

Figure 24. Load vs. Displacement-C15024-*MV* Test Series

Figure 25. Load vs. Displacement-C15015-*M* Test Series

Figure 26. Load vs. Displacement-C15019-*M* Test Series

Figure 27. Load vs. Displacement-C15024-*M* Test Series

Figure 28. Load vs. Displacement-C20015-*V* Test Series

Figure 29. Load vs. Displacement-C20019-*V* Test Series

Figure 30. Load vs. Displacement-C20024-*V* Test Series

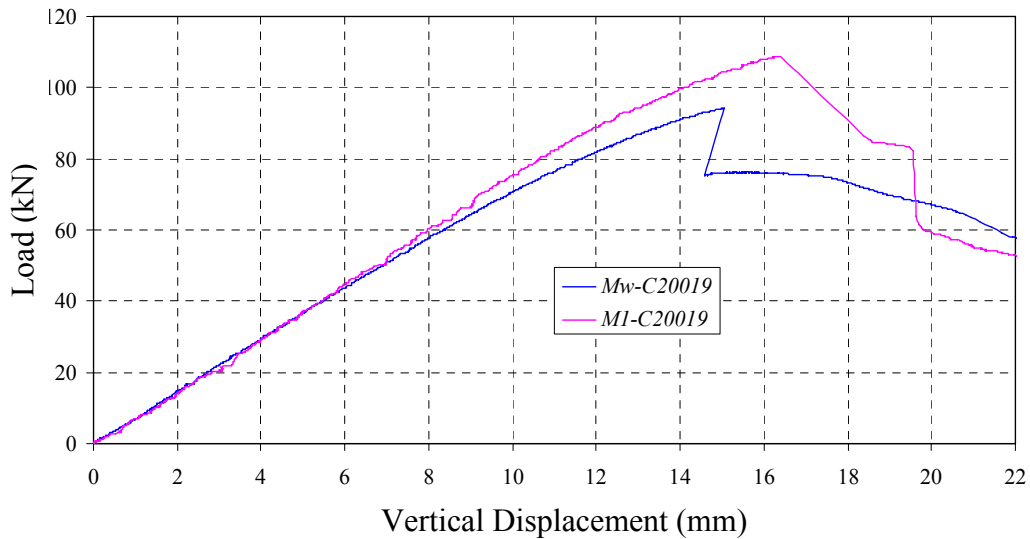Figure 31. Load vs. Displacement-C20015-*MV* Test Series

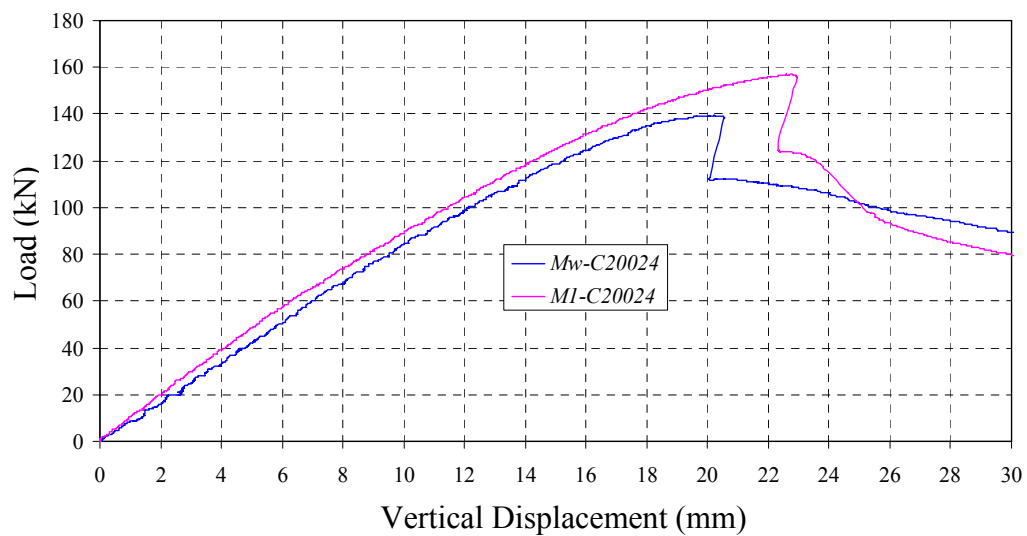Figure 32. Load vs. Displacement-C20019-*MV* Test Series

Figure 33. Load vs. Displacement-C20024-*MV* Test Series

Figure 34. Load vs. Displacement-C20015-*M* Test Series

Figure 35. Load vs. Displacement-C20019-*M* Test Series

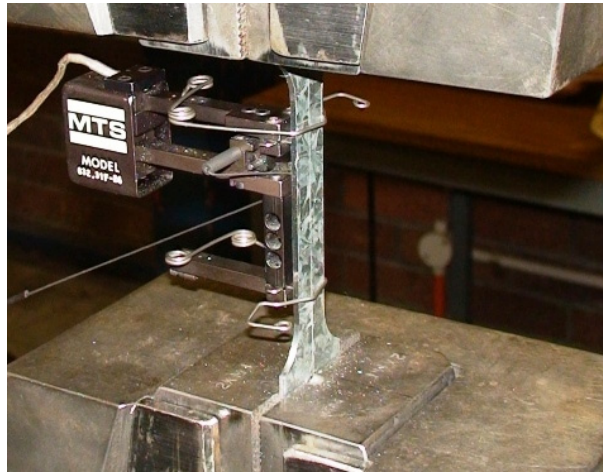Figure 36. Load vs. Displacement-C20024-*M* Test Series

Figure 37. Coupon Test
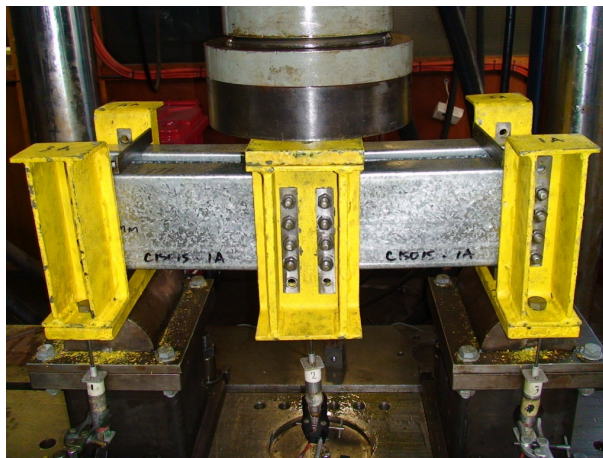

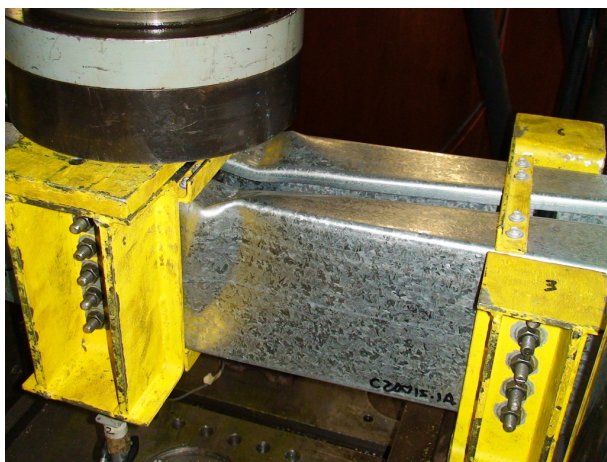Figure 38. *MV* Test Configuration

Figure 39. *M* Test Configuration

Figure 40. *V* Test Series Buckling Mode Shape

(a) With Straps   (b) Without Straps

Figure 41. *MV* Test Series Buckling Mode Shape

(a) With Straps   (b) Without Straps

Figure 42. *M* Test Series Buckling Mode Shape